Mathematical Biosciences and Engineering

http://www.aimspress.com/journal/mbe

MBE, 19(11): 11563–11594.
DOI: 10.3934/mbe.2022539
Received: 20 July 2022
Revised: 31 July 2022
Accepted: 02 August 2022
Published: 12 August 2022

Research article

Novel stochastic dynamics of a fractal-fractional immune effector response to viral infection via latently infectious tissues

Saima Rashid[1,*], Rehana Ashraf[2], Qurat-Ul-Ain Asif[3] and Fahd Jarad[4,5,6,*]

[1] Department of Mathematics, Government College University, Faisalabad 38000, Pakistan
[2] Department of Mathematics, Lahore College for Women University, Lahore, Pakistan
[3] Department of Physics, Government College University, Faisalabad 38000, Pakistan
[4] Department of Mathmatics, Cankaya University, Ankara, Turkey
[5] Department of Medical Research, China Medical University Hospital, China Medical University, Taichung, Taiwan
[6] Department of Mathematics, King Abdulaziz University, Jeddah, Saudi Arabia

* **Correspondence:** Email: saimarashid@gcuf.edu.pk, fahd@cankaya.edu.tr.

Abstract: In this paper, the global complexities of a stochastic virus transmission framework featuring adaptive response and Holling type II estimation are examined via the non-local fractal-fractional derivative operator in the Atangana-Baleanu perspective. Furthermore, we determine the existence-uniqueness of positivity of the appropriate solutions. Ergodicity and stationary distribution of non-negative solutions are carried out. Besides that, the infection progresses in the sense of randomization as a consequence of the response fluctuating within the predictive case's equilibria. Additionally, the extinction criteria have been established. To understand the reliability of the findings, simulation studies utilizing the fractal-fractional dynamics of the synthesized trajectory under the Atangana-Baleanu-Caputo derivative incorporating fractional-order α and fractal-dimension $\wp$ have also been addressed. The strength of white noise is significant in the treatment of viral pathogens. The persistence of a stationary distribution can be maintained by white noise of sufficient concentration, whereas the eradication of the infection is aided by white noise of high concentration.

Keywords: immune effector response model; fractal-fractional derivative operator; Brownian motion; ergodicity and stationary distribution

1. Introduction

Diverse viral outbreaks, including those engendered by the human immune compromised virus (HIV) [1], ebola virus [2], acute respiratory syndrome Coronavirus-2 (SARS-CoV-2) [3], dengue

virus [4], nipah virus [5], HBV [6], etc., have been researched utilizing mathematical formulas to describe the within-host nonlinear versatile tendencies. In typical latent infection systems, uncontrolled infections, vulnerable tissues, and attacked cellular responses interact. Additionally, several researchers highlight the phenomenon of incubation by mentioning persistent contamination. The recipient defensive mechanism responds to viral infestation via inherent and monoclonal antibody immunogenicity. Both kinds of reactions can be roughly classified into lytic and nonlytic parts. While nonlytic responder processes prevent viremia by aqueous molecules, lytic responder strategies eliminate afflicted organisms. Innate mechanisms include the ability of autonomous assassin systems to destroy intracellular pathogens and the nonlytic inhibition of viral multiplication by cytokines released by cellular functions. Cytotoxic T lymphocytes (CTLs), which are allergen antibodies, destroy intracellular pathogens while autoantibodies deactivate dispersed viral proteins and prevent the transmission of bacteria to infected macrophages. Furthermore, CD4+ and CD8+ T lymphocytes can produce chemicals that inhibit infectious proliferation (e.g., IFN- and TNF-), (see Figure 1).

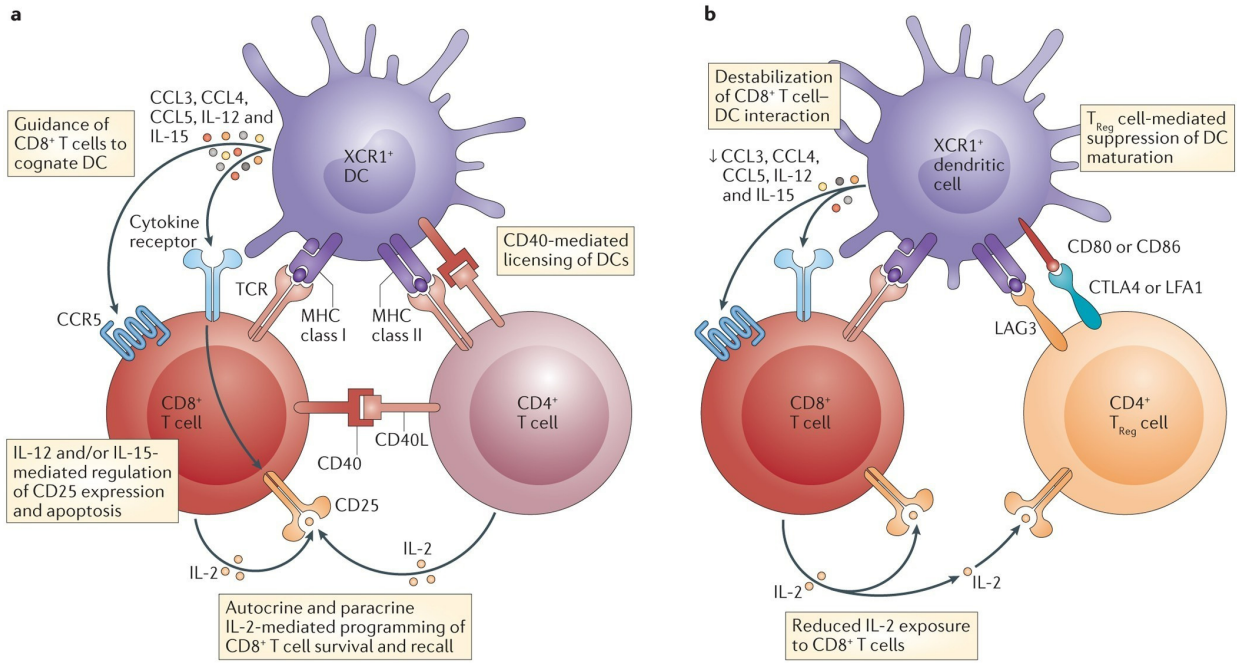

Figure 1. Life cycle of CD4+ and CD8+ T cells.

These discrepancies are not necessarily easy to make, though. For instance, cytokines like interferon and tumour necrotic signal have been shown to promote apoptosis in some circumstances, in addition to inhibiting infectious multiplication [7]. Eichelberger et al. [8] investigated whether the pathogen can be eradicated by the CD4+ T-cell-dependent antigen reaction in the absence of CD8+ T cells, (see Figure 2). Topham et al. [9] demonstrated that CD8+ T lymphocytes can eliminate the pathogen by a lytic process that is either regulated by complement activation or Fas. In terms of explaining the four distinct HCV scenarios quantitatively, Pan et al. [10] addressed the HCV infectious system, which incorporates the pathways of contamination and propagation, such as infectious agent and cell-to-cell dissemination patterns.

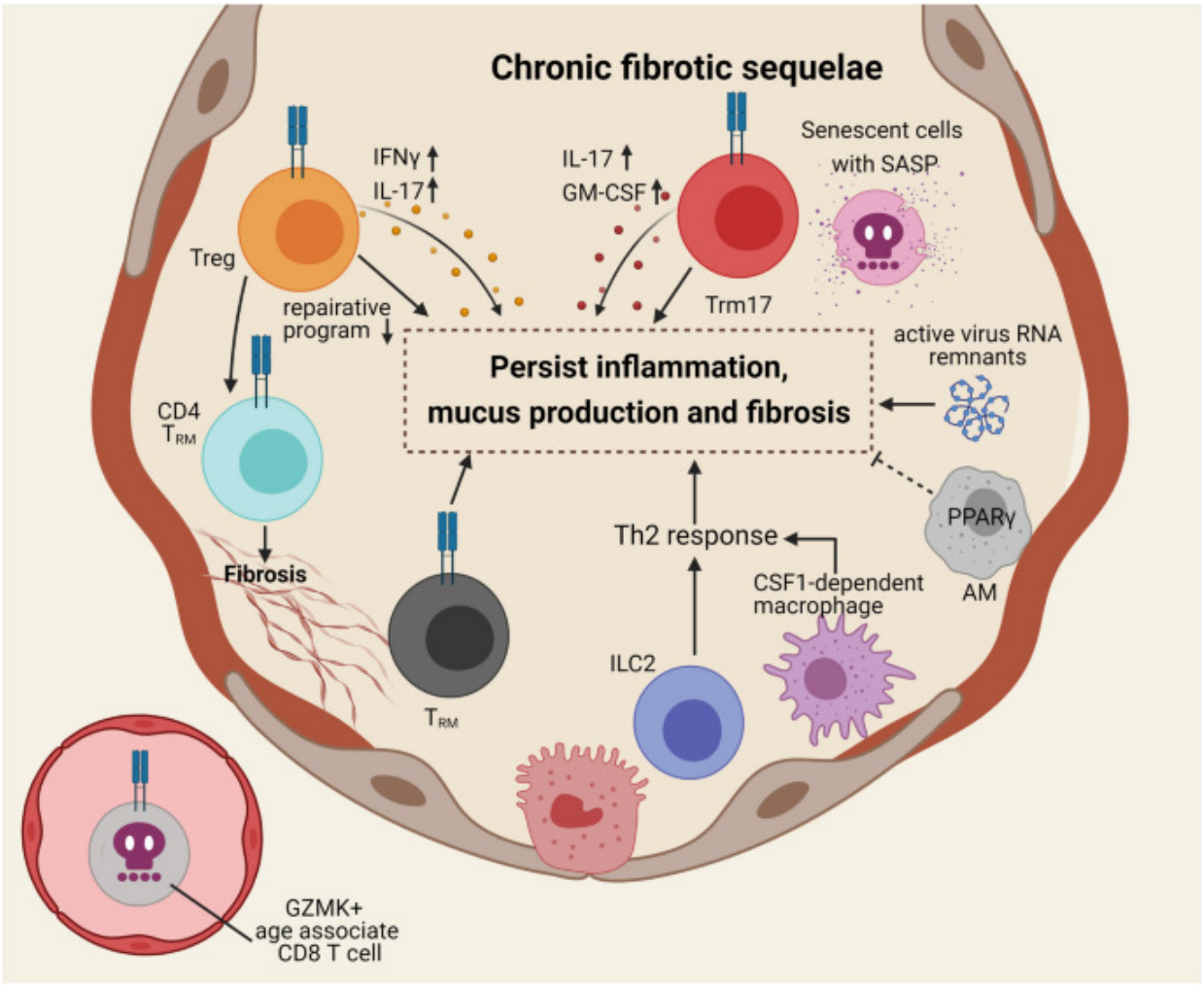

Figure 2. Aging and respiratory viral infection: from acute morbidity to chronic.

Chronic infestations result when the pathogen weakens and suppresses the innate immunity. An immunological reaction has occurred whereby, upon a bacteria's penetration into the system, the immunological mechanism identifies the onslaught and communicates this information to the defensive components, which then generate lymphocytes to eradicate the infection. Additionally, the responsive immunological mechanism is very important in regulating the virus replication. When an infection propagates in a person, the cells respond in two ways: first, a host antibody immune reaction is triggered by the B-cell, and then a cytotoxic immunological reaction is induced by the Cytotoxic T Lymphocyte (CTL). According to earlier investigations, the autoimmune disease seems to be more robust than the intracellular immunological defences. Elaiw et al. [11] addressed the production of antibodies, particular nonlinear prevalence rate expression, and behavioural features of viral transmission scenarios, including insidiously viral particles. Luo et al. [12] analyzed a nonlinear prevalence, cell-to-cell dissemination, and host immune protection framework for diffusive pathogen infectious diseases. Wang et al. [13] investigated the infectious patterns of a system of persistent HIV transmission that included multiple latencies, B-cell immunological responses, and the Beddington-DeAngelis occurrence criterion. Hattaf [14] presented a generalised virus-induced framework with several delayed and

immune regulatory components that exhibit global stability and Hopf bifurcation. Rajivganthi and Rihan [15] presented the stochastic analysis of viral infection model involving latently infected cells. Olaide et al. [16] presented a novel metaheuristic algorithm named ebola optimization search algorithm (EOSA) based on the propagation mechanism of the ebola virus disease. For further investigations on optimization and epidemics, we refer the readers [17–25].

Fractional calculus (FC) is a subfield of mathematics that was created by applying integer derivatives to differential equations (DEs) involving fractional-orders [26–31]. Since many considerable anomalies in digital circuits, phonics, physio-chemical processes, special relativity, photo-catalysis, transport phenomena, stretchability, and optoelectronics can be characterized by fractional DEs, this field, which deals with classical derivatives and fractional-order, has gained popularity in the last three decades. Additionally, FC is currently an essential strategy for simulating complicated events as well as electron mobility that occurs in permeable heterogeneity environments [32–36]. In order to analyze FDEs, scientists require a powerful toolset, yet it might be challenging to identify precise alternatives to these kinds of computations. Therefore, it is vital to designing appropriate quantitative strategies to address these issues [37]. However, quantitative approaches for FDEs create mathematical challenges that are not present in the evaluation of integer-order models. Because certain of the advantageous aspects of the conventional approximation operators are compromised, there are certain systemic problems in performing simulations of the fractional derivatives. During the last decade, the Atangana-Baleanu fractional operator has made recent advancements in fractional DEs approximation, [38]. Atangana [39] proposed a revolutionary nonlocal formulation that combines fractional-order and fractal-dimension: fractal-fractional (FF) differential and integral operators. To examine intricate real-world situations that can never be modelled using classical and fractional derivative/integral formulations of single order, the F-F technique has been expounded as a valuable technique in numerous scientific and epidemiological fields. Versaci et al. [40] presented a fuzzy similarity-based approach to classify numerically simulated and experimentally detected carbon fiber-reinforced polymer plate defects. The present scheme can be further formulated with the method proposed by [40].

However, the fractional-order and integer-order mathematical models have been developed to analyze a large number of randomized order derivatives, providing an additional level of flexibility in selecting; see [41–44]. The stochastic DEs might offer a significant level of reliability, and when linked to deterministic systems, they encompass the comprehensive spectra of an individual cohort and produce a highly precise result as compared to a classical model. We need to execute the simulations repeatedly and detect commonalities in the projected scenarios because the results of every inquiry in a stochastic procedure differ from the preceding [46–48]. According to several researchers, a non-linear recurrence projection for stochastic processes is one of the epidemiological techniques that has been examined for stability evaluation. In fact, random events are prevalent worldwide. Systems frequently experience random disturbances. Various studies have been conducted on stochastic dynamics; for example, a wide range of scientific theories, including meteorology, accounting, biology, and telecommunication systems, frequently exhibit randomized fluctuations with long-term dependency. In order to analyze fractional stochastic processes, fractional Brownian motion (BM) employing the Hurst index $H(1/2, 1)$ has been proposed as an alternative to classical BM [49]. Kerboua et al. [50] looked into stochastic fractional DEs with perturbed regulatory frameworks that involved fractional BM. Pei and Xu [51] investigated the non-Lipschitz stochastic DEs driven by fractional BM. In 2021, authors [52] presented a novel notion for analyzing and predicting the transmission of COVID-19 throughout Africa and Eu-

rope using stochastic and deterministic methods. Alkahtani and Koca [53] contemplated the fractional stochastic SIR system within the fractional calculus technique. Rashid et al. [54] contemplated the stochastic fractal-fractional tuberculosis model via a non-singular kernel with random densities.

Owing to the aforesaid propensity, we intend to suggest a novel fractal-fractional stochastic immune effector response to viral infections while taking the notion of a fluctuating population with white noise into consideration. We intend to divide the entire population into five distinct groups based on the severity of viral infection. Furthermore, several qualitative analyses are conducted, such as the existence and distinctiveness of the positive solution in the stochastic immune effector responses considering a Holling type II functionality reaction. Perceptions from these systems are distilled in this assessment, which also contrasts them with test findings. Numerical results are presented by employing the revolutionary technique proposed by Atangana and Araz [52] in the fractal-fractional derivative sense. Graphical illustrations are presented with low random densities, incorporating the fractal-dimension and fractional-order. In a nutshell, we presented the simulation findings with and without control.

The rest of this paper is structured as follows. Section 2 gives some foundational information on F-F operators in the ABC sense, formulations of stochastic perturbation and the fractional viral infection model construction. In Section 3, we demonstrate the model's configuration. Section 4 exhibits the solution's existence-uniqueness, as well as ergodicity and conducts a stationary distribution study on the proposed model. The unique result for the F-F viral model is established utilizing the Atangana-Baleanu sense and standard Brownian motion in Section 5. Furthermore, the discussion of numerical simulations utilizing the novel numerical scheme is provided to analyze the behaviors of the considered model. Finally, we give the conclusion of our paper in the last section.

2. Preliminaries

Before advancing on to the formal description, it is imperative to study certain fundamental F-F operator concepts. Take into account the parameters provided in [39] as well as the functional $\mathbf{v}(\mathbf{t}_1)$, which is continuous and fractal differentiable on $[c, d]$ with fractal-dimension $\wp$ and fractional-order α.

Definition 2.1. *([39]) The FF operator of* $\mathbf{v}(\bar{\mathbf{t}})$ *involving the index law kernel in the perspective of Riemann–Liouville (RL) can be described as follows for* $\bar{\mathbf{t}} \in [0, 1]$*:*

$$^{FFP}\mathbf{D}_{0,\bar{\mathbf{t}}}^{\alpha,\wp}(\mathbf{v}(\bar{\mathbf{t}})) = \frac{1}{\Gamma(\mathbf{u}-\alpha)}\frac{d}{d\bar{\mathbf{t}}^{\wp}}\int_0^{\bar{\mathbf{t}}}(\bar{\mathbf{t}}-\mathbf{w})^{\mathbf{u}-\alpha-1}\mathbf{v}(\mathbf{w})d\mathbf{w}, \tag{2.1}$$

where $\frac{d\mathbf{v}(\mathbf{w})}{d\mathbf{w}^{\wp}} = \lim_{\bar{\mathbf{t}}\mapsto\varkappa}\frac{\mathbf{v}(\bar{\mathbf{t}})-\mathbf{v}(\varkappa)}{\bar{\mathbf{t}}^{\wp}-\varkappa^{\wp}}$ *and* $\mathbf{u}-1 < \alpha, \wp \leq \mathbf{u} \in \mathbb{N}$.

Definition 2.2. *([39]) The FF operator of* $\mathbf{v}(\bar{\mathbf{t}})$ *involving the exponential decay kernel in the terms of RL can be described as follows for* $\alpha \in [0, 1]$*:*

$$^{FFE}\mathbf{D}_{0,\bar{\mathbf{t}}}^{\alpha,\wp}(\mathbf{v}(\bar{\mathbf{t}})) = \frac{\mathbb{M}(\alpha)}{1-\alpha}\frac{d}{d\bar{\mathbf{t}}^{\wp}}\int_0^{\bar{\mathbf{t}}}\exp\Big(-\frac{\alpha}{1-\alpha}(\bar{\mathbf{t}}-\varkappa)\Big)\mathbf{v}(\varkappa)d\varkappa, \tag{2.2}$$

such that $\mathbb{M}(0) = \mathbb{M}(1) = 1$ *containing* $\alpha > 0,\ \wp \leq \mathbf{u} \in \mathbb{N}$.

Definition 2.3. *([39]) The FF operator of* $\mathbf{v}(\bar{\mathbf{t}})$ *involving the generalized Mittag-Leffler kernel in the perspective of RL can be described as follows for* $\alpha \in [0,1]$*:*

$$^{FFM}\mathbf{D}^{\alpha,\wp}_{0,\bar{\mathbf{t}}}(\mathbf{v}(\bar{\mathbf{t}})) = \frac{\mathbf{ABC}(\alpha)}{1-\alpha}\frac{d}{d\bar{\mathbf{t}}^{\wp}}\int_0^{\bar{\mathbf{t}}} E_{\alpha}\Big(-\frac{\alpha}{1-\alpha}(\bar{\mathbf{t}}-\varkappa)\Big)\mathbf{v}(\varkappa)d\varkappa, \tag{2.3}$$

such that $\mathbf{ABC}(\alpha) = 1-\alpha+\frac{\alpha}{\Gamma(\alpha)}$ *involving* $\alpha > 0,\ \wp \leq 1 \in \mathbb{N}$.

Definition 2.4. *([39]) The corresponding F-F integral formulae of* (2.1) *is described as:*

$$^{FFP}\mathbb{J}^{\alpha}_{0,\bar{\mathbf{t}}}(\mathbf{v}(\bar{\mathbf{t}})) = \frac{\wp}{\Gamma(\alpha)}\int_0^{\bar{\mathbf{t}}}(\bar{\mathbf{t}}-\varkappa)^{\alpha-1}\varkappa^{\wp-1}\mathbf{v}(\varkappa)d\varkappa. \tag{2.4}$$

Definition 2.5. *([39]) The corresponding F-F integral formulae of* (2.2) *is described as:*

$$^{FFE}\mathbb{J}^{\alpha}_{0,\bar{\mathbf{t}}}(\mathbf{v}(\bar{\mathbf{t}})) = \frac{\alpha\wp}{\mathbb{M}(\alpha)}\int_0^{\bar{\mathbf{t}}}\varkappa^{\wp-1}\mathbf{v}(\varkappa)d\varkappa + \frac{\wp(1-\alpha)\bar{\mathbf{t}}^{\wp-1}\mathbf{v}(\bar{\mathbf{t}})}{\mathbb{M}(\alpha)}. \tag{2.5}$$

Definition 2.6. *([39]) The corresponding F-F integral formulae of* (2.3) *is described as:*

$$^{FFM}\mathbb{J}^{\alpha}_{0,\bar{\mathbf{t}}}(\mathbf{v}(\bar{\mathbf{t}})) = \frac{\alpha\wp}{\mathbf{ABC}(\alpha)}\int_0^{\bar{\mathbf{t}}}\varkappa^{\wp-1}(\bar{\mathbf{t}}-\varkappa)^{\alpha-1}\mathbf{v}(\varkappa)d\varkappa + \frac{\wp(1-\alpha)\bar{\mathbf{t}}^{\wp-1}\mathbf{v}(\bar{\mathbf{t}})}{\mathbf{ABC}(\alpha)}. \tag{2.6}$$

Definition 2.7. *([38]) Let* $\mathbf{v} \in H^1(\mathbf{c},\mathbf{d}),\ \ \mathbf{c} < \mathbf{d}$ *and the Atangana-Baleanu fractional derivative operator is described as:*

$$^{ABC}_{\mathbf{c}}\mathbf{D}^{\alpha}_{\bar{\mathbf{t}}}(\mathbf{v}(\bar{\mathbf{t}})) = \frac{\mathbf{ABC}(\alpha)}{1-\alpha}\int_{\mathbf{c}}^{\bar{\mathbf{t}}}\mathbf{v}'(\varkappa)E_{\alpha}\Big(-\frac{\alpha(\bar{\mathbf{t}}-\varkappa)^{\alpha}}{1-\alpha}\Big)d\varkappa,\ \ \alpha \in [0,1], \tag{2.7}$$

where $\mathbf{ABC}(\alpha)$ *represents the normalization function.*

Definition 2.8. *([55]) The Gaussian hypergeometric function* ${}_2\mathcal{F}_1$*, characterized as*

$${}_2\mathcal{F}_1(y_1,y_2;y_3,y_4) = \frac{1}{\mathbb{B}(y_2,y_3-y_2)}\int_1^1 \bar{\mathbf{t}}^{y_2-1}(1-\bar{\mathbf{t}})^{y_3-y_2-1}(1-y_4\bar{\mathbf{t}})^{-y_1}d\bar{\mathbf{t}},\ \ (y_3 > y_2 > 0, |y_1| < 1), \tag{2.8}$$

where $\mathbb{B}(y_1,y_2) = \frac{\Gamma(y_1)\Gamma(y_2)}{\Gamma(y_1+y_2)}$ *and* $\Gamma(y_1) = \int_0^{\infty}\exp(-\bar{\mathbf{t}})\bar{\mathbf{t}}^{y_1}d\bar{\mathbf{t}}$ *is the Gamma function.*

3. Model configuration

Here, the immunological mechanism is necessary for the highly contagious viral replication. If infectious processes are adequately described, the infection and the therapeutic medications employed to address it can be comprehended. Lymphocytes are vicariously liable for specialization and retention in responsive immunological systems. B cells and T cells are the two primary categories of lymphocytes. T cells have the ability to identify and eliminate contaminated organisms, whereas B cells are responsible for producing antigens that can neutralize pathogens. Immune systems, including CTL and antigen-response, have been examined in terms of their impact [56, 57]. The impact of CTL reactions and cytoplasmic latencies has been considered by a few other scientists as well [58]. Murase et al. [59] presented the mathematical framework that shows how adaptive immunity affects viral transmission as follows:

$$\begin{cases} \frac{\mathbf{U}(\bar{\mathbf{t}})}{d\bar{\mathbf{t}}} = \Lambda - \varsigma\mathbf{U}(\bar{\mathbf{t}}) - \lambda_{11}\mathbf{U}(\bar{\mathbf{t}})\mathbf{F}(\bar{\mathbf{t}}) - \lambda_{22}\mathbf{U}(\bar{\mathbf{t}})\mathbf{A}(\bar{\mathbf{t}}), \\ \frac{\mathbf{A}(\bar{\mathbf{t}})}{d\bar{\mathbf{t}}} = \lambda_1\mathbf{U}(\bar{\mathbf{t}})\mathbf{F}(\bar{\mathbf{t}}) + \lambda_2\mathbf{U}(\bar{\mathbf{t}})\mathbf{A}(\bar{\mathbf{t}}) - \delta\mathbf{A}(\bar{\mathbf{t}}), \\ \frac{\mathbf{F}(\bar{\mathbf{t}})}{d\bar{\mathbf{t}}} = \varphi\mathbf{A}(\bar{\mathbf{t}}) - \nu_2\mathbf{F}(\bar{\mathbf{t}}) - \xi\mathbf{F}(\bar{\mathbf{t}})\mathbf{Q}(\bar{\mathbf{t}}), \\ \frac{\mathbf{Q}(\bar{\mathbf{t}})}{d\bar{\mathbf{t}}} = \chi\mathbf{F}(\bar{\mathbf{t}})\mathbf{Q}(\bar{\mathbf{t}}) - \zeta\mathbf{Q}(\bar{\mathbf{t}})\mathbf{A}(\bar{\mathbf{t}}) - \delta\mathbf{A}(\bar{\mathbf{t}}), \end{cases} \tag{3.1}$$

The system (3.1) based on unrestricted infections $\mathbf{F}(\bar{\mathbf{t}})$, unaffected target cells $\mathbf{U}(\bar{\mathbf{t}})$, productively infectious specific cells $\mathbf{A}(\bar{\mathbf{t}})$ and antibodies/B tissue $\mathbf{Q}(\bar{\mathbf{t}})$. The productivity Λ of the infectious organisms $\mathbf{U}(\bar{\mathbf{t}})$ and fatality rate ς are both constant. The incidence of the disease by uncontrolled pathogen is λ_{11}, and uncontrolled bacteria become constructively contaminated at a rate of λ_{22} for each of the two individuals. The percentage of viral components that died at δ, ν_2 and ζ released pathogens, antibodies, and B tissues, respectively. When tissues are actively infested, individual viral particles are created at a speed of φ, where is the ratio ξ at which responses can eliminate the pathogen. The frequency of responses that are active versus the pathogen is χ.

However, the persistent infectious factor is applied to framework (3.1) in this article as an improvement. We suppose that the incidence at which a Holling type II functioning reaction develops is that the unaffected cell $\mathbf{U}(\bar{\mathbf{t}})$ becomes contaminated by a neutral pathogen $\mathbf{F}(\bar{\mathbf{t}})$ or by virus is transmitted organism $\mathbf{A}(\bar{\mathbf{t}})$ at the rate $\frac{\lambda_1\mathbf{U}(\bar{\mathbf{t}})\mathbf{F}(\bar{\mathbf{t}})}{1+\mathbf{F}(\bar{\mathbf{t}})} + \frac{\lambda_2\mathbf{U}(\bar{\mathbf{t}})\mathbf{A}(\bar{\mathbf{t}})}{1+\mathbf{A}(\bar{\mathbf{t}})}$ response. The rates of pathogen to tissue infection and tissue to cell propagation are indicated by $\lambda_1 > 0$ and $\lambda_2 > 0$, , respectively, see [60]. We further estimate that the amounts of contamination that result in response times and efficiency are $1 - \phi$ and $\phi \in (0, 1)$, respectively. In addition, we included the effect of unpredictability within the host by injecting nonlinear disturbances on the spontaneous mortality rate, employing white noise throughout each expression in an attempt to depict a more accurate state of pathogen progression. As a result, the modified framework is specified:

$$\begin{cases} d\mathbf{U}(\bar{\mathbf{t}}) = \Big(\Lambda - \varsigma\mathbf{U}(\bar{\mathbf{t}}) - \frac{\lambda_1\mathbf{U}(\bar{\mathbf{t}})\mathbf{S}(\bar{\mathbf{t}})}{1+\mathbf{S}(\bar{\mathbf{t}})} - \frac{\lambda_2\mathbf{U}(\bar{\mathbf{t}})\mathbf{A}(\bar{\mathbf{t}})}{1+\mathbf{A}(\bar{\mathbf{t}})}\Big)d\bar{\mathbf{t}} + \rho_1\mathbf{U}(\bar{\mathbf{t}})d\mathbf{B}_1(\bar{\mathbf{t}}), \\ d\mathbf{S}(\bar{\mathbf{t}}) = \Big((1-\phi)\Big(\frac{\lambda_1\mathbf{U}(\bar{\mathbf{t}})\mathbf{S}(\bar{\mathbf{t}})}{1+\mathbf{S}(\bar{\mathbf{t}})} + \frac{\lambda_2\mathbf{U}(\bar{\mathbf{t}})\mathbf{A}(\bar{\mathbf{t}})}{1+\mathbf{A}(\bar{\mathbf{t}})}\Big) - (\nu_1+\sigma)\mathbf{S}(\bar{\mathbf{t}})\Big)d\bar{\mathbf{t}} + \rho_2\mathbf{S}(\bar{\mathbf{t}})d\mathbf{B}_2(\bar{\mathbf{t}}), \\ d\mathbf{A}(\bar{\mathbf{t}}) = \Big(\phi\Big(\frac{\lambda_1\mathbf{U}(\bar{\mathbf{t}})\mathbf{S}(\bar{\mathbf{t}})}{1+\mathbf{S}(\bar{\mathbf{t}})} + \frac{\lambda_2\mathbf{U}(\bar{\mathbf{t}})\mathbf{A}(\bar{\mathbf{t}})}{1+\mathbf{A}(\bar{\mathbf{t}})}\Big) + \sigma\mathbf{S}(\bar{\mathbf{t}}) - \delta\mathbf{A}(\bar{\mathbf{t}})\Big)d\bar{\mathbf{t}} + \rho_3\mathbf{A}(\bar{\mathbf{t}})d\mathbf{B}_3(\bar{\mathbf{t}}), \\ d\mathbf{F}(\bar{\mathbf{t}}) = \Big(\varphi\mathbf{A}(\bar{\mathbf{t}}) - \nu_2\mathbf{F}(\bar{\mathbf{t}}) - \xi\mathbf{F}(\bar{\mathbf{t}})\mathbf{Q}(\bar{\mathbf{t}})\Big)d\bar{\mathbf{t}} + \rho_4\mathbf{F}(\bar{\mathbf{t}})d\mathbf{B}_4(\bar{\mathbf{t}}), \\ d\mathbf{Q}(\bar{\mathbf{t}}) = \Big(\chi\mathbf{F}(\bar{\mathbf{t}})\mathbf{Q}(\bar{\mathbf{t}}) - \zeta\mathbf{Q}(\bar{\mathbf{t}})\Big)d\bar{\mathbf{t}} + \rho_5\mathbf{Q}(\bar{\mathbf{t}})d\mathbf{B}_5(\bar{\mathbf{t}}), \end{cases} \tag{3.2}$$

subject to initial conditions (ICs) $\mathbf{U}(0) > 0$, $\mathbf{S}(0) > 0$, $\mathbf{A}(0) > 0$, $\mathbf{F}(0) > 0$, $\mathbf{Q}(0) > 0$. Moreover, the term $\mathbf{S}(\bar{\mathbf{t}})$ stands for the concentrations of contaminated tissues in the predictive phase at time $\bar{\mathbf{t}}$. ν_1 be the death rate of $\mathbf{S}(\bar{\mathbf{t}})$, the underlying contamination becomes prolific at the rate σ. Also, ρ_ι^2, $\iota = 1, ..., 5$ are intensities of standard Gaussian white noise and B_ι, $\iota = 1, ..., 5$ are independent standard Brownian motion (BM). The underlying ideas of probability theory and stochastic differential equations are described as: let $(\Omega, \mathfrak{F}, \{\mathfrak{F}\}_{\bar{\mathbf{t}}\geq 0}, P)$ be a complete probability space using filtration such that $\{\mathfrak{F}\}_{\bar{\mathbf{t}}\geq 0}$ admits the basic requirements. For further information on Itô's technique, see [61]. However, the deterministic model has certain limitations because it cannot consider demographic stochasticity, which are important features of any natural system. Due to the influence of environmental noise, population density usually does not stabilize at a fixed value, but fluctuates around a certain average value. Nowadays, stochastic biological modeling has attracted great interest from researchers all over the world [20–22].

4. Existence-uniqueness of non-negative solution

In what follows, we provide the accompanying result to identify the stochastic model's (3.2) existence and uniqueness.

Theorem 4.1. *For* $\chi < \xi < \zeta$, $\lambda_1\varphi < \nu_2 + \chi, 1 + \lambda_2 < \frac{\delta}{\varphi}$, *the solution of the system* (3.2) $(\mathbf{U}(0), \mathbf{S}(0), \mathbf{A}(0), \mathbf{F}(0), \mathbf{Q}(0))$ *is unique for* $\bar{\mathbf{t}} \geq 0$ *underlying ICs* $(\mathbf{U}(0), \mathbf{S}(0), \mathbf{A}(0), \mathbf{F}(0), \mathbf{Q}(0)) \in \mathbb{R}_+^5$. *Also, the solution will probably stay in* $\mathbb{R}_+^5$ *having unit probability, i,e.,* $(\mathbf{U}(0), \mathbf{S}(0), \mathbf{A}(0), \mathbf{F}(0), \mathbf{Q}(0)) \in \mathbb{R}_+^5$, $\forall\, \bar{\mathbf{t}} > 0$ *almost surely (a.s).*

Proof. Briefly, if the local Lipschitz criterion is fulfilled by the components of the scheme (3.2). Thus, (3.2) has an unique local solution $(\mathbf{U}(\bar{\mathbf{t}}), \mathbf{S}(\bar{\mathbf{t}}), \mathbf{A}(\bar{\mathbf{t}}), \mathbf{F}(\bar{\mathbf{t}}), \mathbf{Q}(\bar{\mathbf{t}}))$ on $[0, \tau_e]$, where τ_e is the exposition duration. Then, we illustrate that $\tau_e = \infty$. Let us apply the same methodology used in [48] to prove the result. Our intention is to define a non-negative mapping $\mathbb{C}^2$ as $\mathcal{H} : \mathbb{R}_+^5 \mapsto \mathbb{R}_+$ such that $\lim_{\eta\mapsto\infty}(\mathbf{U}(\bar{\mathbf{t}}), \mathbf{S}(\bar{\mathbf{t}}), \mathbf{A}(\bar{\mathbf{t}}), \mathbf{F}(\bar{\mathbf{t}}), \mathbf{Q}(\bar{\mathbf{t}})) \in \mathbb{R}_+^5 \backslash \Upsilon_\eta \inf \mathcal{H}(\mathbf{U}, \mathbf{S}, \mathbf{A}, \mathbf{F}, \mathbf{Q}) = \infty$ and $\mathbb{L}\mathcal{H}(\mathbf{U}, \mathbf{S}, \mathbf{A}, \mathbf{F}, \mathbf{Q}) \leq \Bbbk$, where $\Upsilon_\eta = (1/\eta, \eta) \times (1/\eta, \eta) \times (1/\eta, \eta) \times (1/\eta, \eta) \times (1/\eta, \eta)$ and $\Bbbk$ is non-negative constant.
Now, considering two positive constants values ϵ from $(0, 1)$ and $\mathbb{T}$ must exist such that

$$P[\mathbb{T} \geq \tau_\infty] > \epsilon. \tag{4.1}$$

Introducing a mapping $\mathcal{H} : \mathbb{R}_+^5 \mapsto \mathbb{R}_+$ as:

$$\mathcal{H}(\mathbf{U}, \mathbf{S}, \mathbf{A}, \mathbf{F}, \mathbf{Q}) = \mathbf{U} + \mathbf{S} + \mathbf{A} + \mathbf{F} + \mathbf{Q} - 5 - (\ln \mathbf{U} + \ln \mathbf{S} + \ln \mathbf{A} + \ln \mathbf{F} + \ln \mathbf{Q}). \tag{4.2}$$

This stored procedure non-negativity is shown by examining at $\varrho - 1 \ln \varrho$, $\forall \varrho > 0$. Suppose that $\Bbbk_0 \leq \Bbbk$ and $\mathbb{T} > 0$. The Itô's formula can be used to acquire

$$\begin{aligned} d\mathcal{H}(\mathbf{U}, \mathbf{S}, \mathbf{A}, \mathbf{F}, \mathbf{Q}) \quad &= \mathbb{L}\mathcal{H}(\mathbf{U}, \mathbf{S}, \mathbf{A}, \mathbf{F}, \mathbf{Q})d\bar{\mathbf{t}} + \rho_1(\mathbf{U} - 1)d\mathbf{B}_1(\bar{\mathbf{t}}) + \rho_2(\mathbf{S} - 1)d\mathbf{B}_2(\bar{\mathbf{t}}) \\ &\quad + \rho_3(\mathbf{A} - 1)d\mathbf{B}_3(\bar{\mathbf{t}}) + \rho_4(\mathbf{F} - 1)d\mathbf{B}_4(\bar{\mathbf{t}}) + \rho_5(\mathbf{Q} - 1)d\mathbf{B}_5(\bar{\mathbf{t}}). \end{aligned} \tag{4.3}$$

It follows that

$$\begin{aligned}\mathbb{L}\mathcal{H}(\mathbf{U},\mathbf{S},\mathbf{A},\mathbf{F},\mathbf{Q}) &= \Big(1-\frac{1}{\mathbf{U}}\Big)\Big(\Lambda-\varsigma\mathbf{U}(\bar{\mathbf{t}})-\frac{\lambda_1\mathbf{U}(\bar{\mathbf{t}})\mathbf{S}(\bar{\mathbf{t}})}{1+\mathbf{S}(\bar{\mathbf{t}})}-\frac{\lambda_2\mathbf{U}(\bar{\mathbf{t}})\mathbf{A}(\bar{\mathbf{t}})}{1+\mathbf{A}(\bar{\mathbf{t}})}\Big)\\ &\quad+\Big(1-\frac{1}{\mathbf{S}}\Big)\Big((1-\phi)\Big(\frac{\lambda_1\mathbf{U}(\bar{\mathbf{t}})\mathbf{S}(\bar{\mathbf{t}})}{1+\mathbf{S}(\bar{\mathbf{t}})}+\frac{\lambda_2\mathbf{U}(\bar{\mathbf{t}})\mathbf{A}(\bar{\mathbf{t}})}{1+\mathbf{A}(\bar{\mathbf{t}})}\Big)-(\nu_1+\sigma)\mathbf{S}(\bar{\mathbf{t}})\Big)\\ &\quad+\Big(1-\frac{1}{\mathbf{A}}\Big)\Big(\phi\Big(\frac{\lambda_1\mathbf{U}(\bar{\mathbf{t}})\mathbf{S}(\bar{\mathbf{t}})}{1+\mathbf{S}(\bar{\mathbf{t}})}+\frac{\lambda_2\mathbf{U}(\bar{\mathbf{t}})\mathbf{A}(\bar{\mathbf{t}})}{1+\mathbf{A}(\bar{\mathbf{t}})}\Big)\\ &\quad+\Big(1-\frac{1}{\mathbf{F}}\Big)\Big(\varphi\mathbf{A}(\bar{\mathbf{t}})-\nu_2\mathbf{F}(\bar{\mathbf{t}})-\xi\mathbf{F}(\bar{\mathbf{t}})\mathbf{Q}(\bar{\mathbf{t}})\Big)\\ &\quad+\Big(1-\frac{1}{\mathbf{Q}}\Big)\Big(\chi\mathbf{F}(\bar{\mathbf{t}})\mathbf{Q}(\bar{\mathbf{t}})-\zeta\mathbf{Q}(\bar{\mathbf{t}})\Big)\\ &\leq \frac{1}{2}(\rho_1^2+\rho_2^2+\rho_3^2+\rho_4^2+\rho_5^2)+\Lambda+\varsigma+\nu_1+\sigma_1+\delta+\nu_2+\zeta\\ &\quad+((\xi-\zeta)+(\chi-\xi)\mathbf{F})\mathbf{Q}+(\lambda\varphi-(\nu_2+\chi))\mathbf{F}+((\lambda_2+1)\varphi-\delta)\mathbf{A}. \quad (4.4)\end{aligned}$$

Utilizing the given hypothesis, there exists a non-negative constant η such that $\mathbb{L}\mathcal{H}<\eta$.
Therefore,

$$\begin{aligned}&\mathbb{U}\Big[\mathcal{H}(\mathbf{U}(\tau_\eta\wedge\mathbb{T}),\mathbf{S}(\tau_\eta\wedge\mathbb{T}),\mathbf{A}(\tau_\eta\wedge\mathbb{T}),\mathbf{F}(\tau_\eta\wedge\mathbb{T}),\mathbf{Q}(\tau_\eta\wedge\mathbb{T}))\Big]\\ &\leq \mathcal{H}(\mathbf{U}(0),\mathbf{S}(0),\mathbf{A}(0),\mathbf{F}(0),\mathbf{Q}(0))+\mathbb{U}\Big[\int_0^{\tau_\eta\wedge\mathbb{T}}\eta d\bar{\mathbf{t}}\Big]\\ &\leq \mathcal{H}(\mathbf{U}(0),\mathbf{S}(0),\mathbf{A}(0),\mathbf{F}(0),\mathbf{Q}(0))+\eta\mathbb{T}. \quad (4.5)\end{aligned}$$

Inserting $\Omega_\eta=\{\tau_\eta\leq\mathbb{T}\}$ for $\eta\geq\eta_1$ and by (4.1) we have $P(\Omega_\eta)\geq\epsilon$. Observe that for every ω from Ω_η there exist at least one $\mathbf{U}(\tau_\eta,\omega),\mathbf{S}(\tau_\eta,\omega),\mathbf{A}(\tau_\eta,\omega),\mathbf{F}(\tau_\eta,\omega),\mathbf{Q}(\tau_\eta,\omega)$ that yields $1/\eta$ *or* η. Consequently, $\mathcal{H}(\mathbf{U}(\tau_\eta),\mathbf{S}(\tau_\eta),\mathbf{A}(\tau_\eta),\mathbf{F}(\tau_\eta),\mathbf{Q}(\tau_\eta))\geq\Big(1/\eta-1+\ln\eta\Big)\wedge\mathbb{U}(\eta-1-\ln\eta)$.
In view of (4.1) and (4.5), we can express

$$\begin{aligned}\mathcal{H}(\mathbf{U}(0),\mathbf{S}(0),\mathbf{A}(0),\mathbf{F}(0),\mathbf{Q}(0))+\eta\mathbb{T} &\geq \mathbb{U}\Big[1_{\Omega_{(\omega)}}\mathcal{H}(\mathbf{U}(\tau_\eta),\mathbf{S}(\tau_\eta),\mathbf{A}(\tau_\eta),\mathbf{F}(\tau_\eta),\mathbf{Q}(\tau_\eta))\Big]\\ &\geq \epsilon\Big(1/\eta-1+\ln\eta\Big)\wedge\mathbb{U}(\eta-1-\ln\eta). \quad (4.6)\end{aligned}$$

The indicating mapping of ω is denoted as $1_{\Omega_{(\omega)}}$ that approaches to ∞, the contradiction

$$\infty>\mathcal{H}(\mathbf{U}(0),\mathbf{S}(0),\mathbf{A}(0),\mathbf{F}(0),\mathbf{Q}(0))+\eta\mathbb{T}=\infty$$

reveals itself, proving that $\tau_\infty=\infty$.

4.1. Ergodicity and Stationary distribution (ESD)

Now, we review and examine the model's (3.2) stationary distribution outcomes, which show that the infections are eliminated or enduring.
Suppose there be a regular Markov technique in $\mathbb{R}_+^{\mathfrak{n}}$ for which the behaviour is as below:

$$d\Phi(\bar{\mathbf{t}})=b_1(\Phi)d\bar{\mathbf{t}}+\sum_{r_1}^{\mathbf{u}}\zeta_{r_1}d\Psi_{r_1}(\bar{\mathbf{t}}).$$

The diffusion matrix takes the form

$$\mathbb{A}(\Phi) = [a_{ij}(\phi)], \;\; a_{ij}(\phi) = \sum_{r_1=1}^{\mathbf{u}} \zeta_{r_1}^{i}(\phi)\zeta_{j}^{r_1}(\phi).$$

Lemma 4.1. *([62]) Suppose there is a unique stationary distribution technique* $\Phi(\bar{\mathbf{t}})$. *If there is a bounded region involving regular boundary such that* $S, \bar{S} \in \mathbb{R}^d \bar{S}$ *closure* $\bar{S} \in \mathbb{R}^d$ *satisfies the following:*
(a) *The smallest eigenvalue for* $\mathbb{A}(\bar{\mathbf{t}})$ *is bounded away from* $(0, 0)$ *for the open region* S *having neighbourhood.*
(b) *For* $\psi \in \mathbb{R}^d S$, *the mean time* τ *is bounded and for every compact subset* $K \subset \mathbb{R}^{\mathrm{n}}$, $\sup_{\psi\in\Bbbk} S^{\psi}\tau < \infty$. *Therefore,* $f_1(.)$ *is an integrable mapping containing measure* π, *then*

$$P\Big(\lim_{\mathbb{T}\mapsto\infty} \frac{1}{\mathbb{T}} \int_0^{\mathbb{T}} f_1(\Phi_{\psi}(\bar{\mathbf{t}}))d\bar{\mathbf{t}} = \int_{\mathbb{R}^d} f_1(\psi)\pi(d\psi)\Big) = 1, \; \forall \; \psi \in \mathbb{R}^d.$$

Theorem 4.2. *For* $\hat{\sigma} = \nu_1 + \sigma + \frac{\rho_2^2}{2}$, $\hat{\delta} = \delta + \frac{\rho_3^2}{2}$, $\hat{\nu_2} = \nu_2 + \frac{\rho_4^2}{2}$, *then assume that* $\mathbb{R}_0^s := \frac{\Lambda\sigma\varphi\lambda_1(1-\phi)}{\varsigma\hat{\delta}\hat{\sigma}} > 1$, *then for any ICs exists in* $\mathbb{R}_+^5$, *the system has a unique ESD* $\pi(.)$.

Proof. The diffusive matrix for system (3.2) is computed as follows:

$$\mathbb{A} = \begin{bmatrix} \rho_1^2\mathbf{U}^2 & 0 & 0 & 0 & 0 \\ 0 & \rho_2^2\mathbf{S}^2 & 0 & 0 & 0 \\ 0 & 0 & \rho_3^2\mathbf{A}^2 & 0 & 0 \\ 0 & 0 & 0 & \rho_4^2\mathbf{F}^2 & 0 \\ 0 & 0 & 0 & 0 & \rho_5^2\mathbf{U}^2 \end{bmatrix}.$$

This proves that the criteria **(a)** in Lemma 4.1 is applicable for any compact subset of $\mathbb{R}_+^5$. In view of mapping $\mathbb{C}^2$ defined as $\mathcal{H} : \mathbb{R}_+^5 \mapsto \mathbb{R}_+$. Thus, we have

$$\begin{aligned} \mathcal{H}(\mathbf{U}, \mathbf{S}, \mathbf{A}, \mathbf{F}, \mathbf{Q}) \quad &:= \mathcal{M}\Big(\ln\frac{1}{\mathbf{U}} + \ell_1 \ln\frac{1}{\mathbf{S}} + \ell_2 \ln\frac{1}{\mathbf{A}} + \ell_3 \ln\frac{1}{\mathbf{F}} + \ln\frac{1}{\mathbf{Q}}\Big) \\ &\quad + \ln\frac{1}{\mathbf{U}} + \ln\frac{1}{\mathbf{S}} + \ln\frac{1}{\mathbf{A}} + \ln\frac{1}{\mathbf{F}} + \frac{(\mathbf{U}+\mathbf{S}+\mathbf{A}+\mathbf{F}+\mathbf{Q})^{\theta+1}}{\theta+1} \\ &= \mathcal{M}\mathcal{H}_1 + \mathcal{H}_2 + \mathcal{H}_3 + \mathcal{H}_4 + \mathcal{H}_5 + \mathcal{H}_6, \end{aligned}$$

where $\theta \in [0, 1]$, $\ell_1 = \frac{\Lambda\lambda_1\sigma\varphi(1-\phi)}{\hat{\sigma}^2\hat{a}\hat{\nu_2}}$, $\ell_2 = \frac{\Lambda\lambda_1\sigma\varphi(1-\phi)}{\hat{\sigma}^2\hat{a}^2\hat{\nu_2}}$, $\ell_3 = \frac{\Lambda\lambda_1\sigma\varphi}{\hat{\sigma}\hat{a}\hat{\nu_2}^2}$ fulfilling $c - \frac{\theta}{2}(\rho_1^2 \vee \rho_2^2 \vee \rho_3^2 \vee \rho_4^2 \vee \rho_5^2) > 0$ and $\mathcal{M} > 0$, admitting the assumption $-\mathcal{M}\nu_2 + N_1 \leq -2$ and $\nu_2 = \varsigma(\mathbb{R}_0^s - 1) > 0$.
This shows that $\mathcal{H}(\mathbf{U}, \mathbf{S}, \mathbf{A}, \mathbf{F}, \mathbf{Q})$ is continuous as well as it tends to ∞. So that $(\mathbf{U}, \mathbf{S}, \mathbf{A}, \mathbf{F}, \mathbf{Q})$ approaches to $\mathbb{R}_+^5$ and $\|(\mathbf{U}, \mathbf{S}, \mathbf{A}, \mathbf{F}, \mathbf{Q})\| \mapsto \infty$. Also, $\mathcal{H}$ have ICs that lies in $\mathbb{R}_+^5$.
Again, in view of mapping $\mathbb{C}^2$ defined as $\mathcal{H} : \mathbb{R}_+^5 \mapsto \mathbb{R}_+$. Thus, we have

$$\bar{\mathcal{H}}(\mathbf{U}, \mathbf{S}, \mathbf{A}, \mathbf{F}, \mathbf{Q}) = \mathcal{H}\mathbf{U}, \mathbf{S}, \mathbf{A}, \mathbf{F}, \mathbf{Q} - \mathcal{H}(\mathbf{U}(0), \mathbf{S}(0), \mathbf{A}(0), \mathbf{F}(0), \mathbf{Q}(0)).$$

Considering Itô's technique $\mathbb{L}$ on the mappings $\mathcal{H}_1, ..., \mathcal{H}_6$ and utilizing the given hypothesis such that $c = \max\{\varsigma, \nu_1, \delta, \nu_2, \zeta\}$, we have

$$\begin{aligned}\mathbb{L}\mathcal{H}_1 \quad &\leq -\frac{\Lambda}{\mathbf{U}} - \frac{\ell_1}{\mathbf{S}}(1-\phi)\lambda_1\mathbf{U}\mathbf{F} - \frac{\sigma\ell_2\mathbf{S}}{\mathbf{A}} - \frac{\varphi\mathbf{A}\ell_3}{\mathbf{F}} + \varsigma + \lambda_2\mathbf{A} + \ell_1(\nu_1+\sigma) + \delta\ell_2 + \nu_2\ell_3 \\ &\quad +\xi\mathbf{Q}\ell_3 - (\chi-\lambda_1)\mathbf{F} + \zeta + \frac{1}{2}(\rho_1^2 + \ell_1\rho_2^2 + \ell_2\rho_3^2 + \ell_3\rho_4^2 + \rho_4^2) \\ &\leq -\mathbf{F} + \frac{\rho_1^2}{2} + \zeta + \rho_5^2 + \lambda_2\mathbf{A} + \xi\ell_3\mathbf{Q}. \end{aligned} \tag{4.7}$$

Analogously, we have

$$\begin{aligned}\mathbb{L}\mathcal{H}_2 &\leq -\frac{\Lambda}{\mathbf{U}} + \varsigma + \lambda_1\mathbf{F} + \lambda_2\mathbf{A} + \frac{\rho_1^2}{2}, \\ \mathbb{L}\mathcal{H}_3 &= -\frac{1}{\mathbf{S}}(1-\phi)\Big(\frac{\lambda_1\mathbf{U}\mathbf{F}}{1+\mathbf{F}} + \frac{\lambda_2\mathbf{U}\mathbf{A}}{1+\mathbf{A}}\Big) + \nu_1 + \sigma + \frac{\rho_2^2}{2}, \\ \mathbb{L}\mathcal{H}_4 &= -\frac{\phi\lambda_1\mathbf{U}\mathbf{F}}{\mathbf{A}(1+\mathbf{F})} - \frac{\phi\lambda_2\mathbf{U}}{1+\mathbf{A}} - \frac{\sigma\mathbf{S}}{\mathbf{A}} + \delta + \frac{\rho_3^2}{2}, \\ \mathbb{L}\mathcal{H}_5 &= -\frac{\varphi\mathbf{A}}{\mathbf{F}} + \nu_2 + \xi\mathbf{Q} + \frac{\rho_4^2}{2}, \\ \mathbb{L}\mathcal{H}_5 &\leq \mathcal{N}_2 - \frac{1}{2}\Big(c_1 - \frac{\theta}{2}(\rho_1^2 \vee \rho_2^2 \vee \rho_3^2 \vee \rho_4^2 \vee \rho_5^2)\Big)(\mathbf{U}^{\theta+1}, \mathbf{S}^{\theta+1}, \mathbf{A}^{\theta+1}, \mathbf{F}^{\theta+1}, \mathbf{Q}^{\theta+1}), \end{aligned} \tag{4.8}$$

where $\mathcal{N}_2 = \sup_{(\mathbf{U},\mathbf{S},\mathbf{A},\mathbf{F},\mathbf{Q})\in\mathbb{R}_+^5} \Big\{\Lambda(\mathbf{U}+\mathbf{S}+\mathbf{A}+\mathbf{F}+\mathbf{Q})^\theta - \frac{1}{2}\Big(c_1 - \frac{\theta}{2}(\rho_1^2\vee\rho_2^2\vee\rho_3^2\vee\rho_4^2\vee\rho_5^2)\Big)(\mathbf{U}+\mathbf{S}+\mathbf{A}+\mathbf{F}+\mathbf{Q})^{\theta+1}\Big\} < \infty$.
Utilizing (4.7) and (4.8), we have

$$\begin{aligned}\mathbb{L}\bar{\mathcal{H}} \quad &\leq \frac{-\Lambda}{\mathbf{U}} - \mathcal{M}\mathbf{F} + (\mathcal{M}\ell_3 + 1)\xi\mathbf{Q} - \frac{1}{\mathbf{S}}(1-\phi)\lambda_1\mathbf{U}\mathbf{F} - \frac{\phi\lambda_2\mathbf{U}}{1+\mathbf{A}} - \frac{\varphi\mathbf{A}}{\mathbf{F}} \\ &\quad -\frac{1}{2}\Big(c_1 - \frac{\theta}{2}(\rho_1^2 \vee \rho_2^2 \vee \rho_3^2 \vee \rho_4^2 \vee \rho_5^2)\Big)(\mathbf{U}^{\vartheta+1} + \mathbf{S}^{\vartheta+1} + \mathbf{A}^{\vartheta+1} + \mathbf{F}^{\vartheta+1} + \mathbf{Q}^{\vartheta+1}) + \varsigma \\ &\quad +(\mathcal{M}+1)\frac{\rho_1^2}{2} + \mathcal{M}\zeta + \mathcal{M}\frac{\rho_5^2}{2} + (\mathcal{M}+1)\lambda_2\mathbf{A} + \delta + \nu_2 + \lambda_1\mathbf{F} + \mathcal{N}_2 + \nu_1 + \sigma \\ &\quad +\frac{\rho_2^2}{2} + \frac{\rho_3^2}{2} + \frac{\rho_4^2}{2}. \end{aligned} \tag{4.9}$$

For $\epsilon > 0$, we construct the following set

$$\mathbb{D} = \Big\{(\mathbf{U},\mathbf{S},\mathbf{A},\mathbf{F},\mathbf{Q}) \in \mathbb{R}_+^5 : \mathbf{U} \in [\epsilon, 1/\epsilon], \mathbf{S} \in [\epsilon^5, 1/\epsilon^5], \mathbf{A} \in [\epsilon^2, 1/\epsilon^2], \mathbf{F} \in [\epsilon^3, 1/\epsilon^3], \mathbf{Q} \in [\epsilon, 1/\epsilon]\Big\}. \tag{4.10}$$

We can validate Lemma 4.1 in order to demonstrate that $\mathbb{L}\bar{\mathcal{H}} \leq -1$ for $(\mathbf{U},\mathbf{S},\mathbf{A},\mathbf{F},\mathbf{Q}) \in \mathbb{R}_+^5\backslash\mathbb{D}$ *and* $\mathbb{R}_+^5\backslash\mathbb{D} = \bigcup_{\iota=1}^{10}\mathbb{D}_\iota$, where

$$\begin{aligned}\mathbb{D}_1 &= \{(\mathbf{U},\mathbf{S},\mathbf{A},\mathbf{F},\mathbf{Q}) \in \mathbb{R}_+^5 : \mathbf{U} \in (0,\epsilon)\}, \\ \mathbb{D}_2 &= \{(\mathbf{U},\mathbf{S},\mathbf{A},\mathbf{F},\mathbf{Q}) \in \mathbb{R}_+^5 : \mathbf{A} \in (0,\epsilon^5), \mathbf{U} \geq \epsilon, \mathbf{F} \geq \epsilon^3\}, \end{aligned}$$

$$\begin{aligned}
\mathbb{D}_3 &= \{(\mathbf{U},\mathbf{S},\mathbf{A},\mathbf{F},\mathbf{Q}) \in \mathbb{R}^5_+ : \mathbf{A} \in (0,\epsilon^2),\ \mathbf{U} \geq \epsilon\},\\
\mathbb{D}_4 &= \{(\mathbf{U},\mathbf{S},\mathbf{A},\mathbf{F},\mathbf{Q}) \in \mathbb{R}^5_+ : \mathbf{F} \in (0,\epsilon^3), \mathbf{A} \geq \epsilon^2\},\\
\mathbb{D}_5 &= \{(\mathbf{U},\mathbf{S},\mathbf{A},\mathbf{F},\mathbf{Q}) \in \mathbb{R}^5_+ : \mathbf{Q} \in (0,\epsilon)\},\\
\mathbb{D}_6 &= \{(\mathbf{U},\mathbf{S},\mathbf{A},\mathbf{F},\mathbf{Q}) \in \mathbb{R}^5_+ : \mathbf{U} > 1/\epsilon\},\\
\mathbb{D}_7 &= \{(\mathbf{U},\mathbf{S},\mathbf{A},\mathbf{F},\mathbf{Q}) \in \mathbb{R}^5_+ : \mathbf{S} > 1/\epsilon^5\},\\
\mathbb{D}_8 &= \{(\mathbf{U},\mathbf{S},\mathbf{A},\mathbf{F},\mathbf{Q}) \in \mathbb{R}^5_+ : \mathbf{A} > 1/\epsilon^2\},\\
\mathbb{D}_9 &= \{(\mathbf{U},\mathbf{S},\mathbf{A},\mathbf{F},\mathbf{Q}) \in \mathbb{R}^5_+ : \mathbf{F} > 1/\epsilon^3\},\\
\mathbb{D}_{10} &= \{(\mathbf{U},\mathbf{S},\mathbf{A},\mathbf{F},\mathbf{Q}) \in \mathbb{R}^5_+ : \mathbf{Q} > 1/\epsilon\}.
\end{aligned} \tag{4.11}$$

Case (a) If $(\mathbf{U},\mathbf{S},\mathbf{A},\mathbf{F},\mathbf{Q}) \in \mathbb{D}_1$, then by (4.9), we find

$$\begin{aligned}
\mathbb{L}\bar{\mathcal{H}} \quad &\leq \frac{-\Lambda}{\mathbf{U}} + (\mathcal{M}\ell_3 + 1)\xi\mathbf{Q} - \frac{1}{4}\Big(c_1 - \frac{\theta}{2}(\rho_1^2 \vee \rho_2^2 \vee \rho_3^2 \vee \rho_4^2 \vee \rho_5^2)\Big)(\mathbf{U}^{\vartheta+1} + \mathbf{S}^{\vartheta+1} + \mathbf{A}^{\vartheta+1}\\
&\quad + \mathbf{F}^{\vartheta+1} + \mathbf{Q}^{\vartheta+1}) + \varsigma + (\mathcal{M}+1)\frac{\rho_1^2}{2} + \mathcal{M}\zeta + \mathcal{M}\frac{\rho_5^2}{2} + (\mathcal{M}+1)\lambda_2\mathbf{A} + \delta + \nu_2\\
&\quad + \lambda_1\mathbf{F} + \mathcal{N}_2 + \nu_1 + \sigma + \frac{\rho_2^2}{2} + \frac{\rho_3^2}{2} + \frac{\rho_4^2}{2}\\
&\leq -\frac{\Lambda}{\epsilon} + \mathcal{M}_1
\end{aligned} \tag{4.12}$$

If we choose a sufficiently small $\epsilon > 0$, then we get $\mathbb{L}\bar{\mathcal{H}} < 0$ for each $(\mathbf{U},\mathbf{S},\mathbf{A},\mathbf{F},\mathbf{Q}) \in \mathbb{D}_1$.
Case (b) If $(\mathbf{U},\mathbf{S},\mathbf{A},\mathbf{F},\mathbf{Q}) \in \mathbb{D}_2$, then by (4.9), we find

$$\begin{aligned}
\mathbb{L}\bar{\mathcal{H}} \quad &\leq \frac{-1}{\mathbf{S}}(1-\phi)\lambda_1\mathbf{U}\mathbf{F} + \mathcal{M}_1\\
&\leq \frac{-1}{\epsilon}(1-\phi)\lambda_1 + \mathcal{M}_1
\end{aligned}$$

If we choose a sufficiently small $\epsilon^5 > 0$, then we get $\mathbb{L}\bar{\mathcal{H}} < 0$ for each $(\mathbf{U},\mathbf{S},\mathbf{A},\mathbf{F},\mathbf{Q}) \in \mathbb{D}_2$.
Case (c) If $(\mathbf{U},\mathbf{S},\mathbf{A},\mathbf{F},\mathbf{Q}) \in \mathbb{D}_3$, then by (4.9), we find

$$\begin{aligned}
\mathbb{L}\bar{\mathcal{H}} \quad &\leq \frac{-\phi\lambda_2\mathbf{U}}{1+\mathbf{A}} + \mathcal{M}_1\\
&\leq \frac{-\phi\lambda_2\epsilon}{1+\epsilon^2} + \mathcal{M}_1.
\end{aligned}$$

If we choose a sufficiently small $\epsilon^2 > 0$, then we get $\mathbb{L}\bar{\mathcal{H}} < 0$ for each $(\mathbf{U},\mathbf{S},\mathbf{A},\mathbf{F},\mathbf{Q}) \in \mathbb{D}_3$.
Case (d) If $(\mathbf{U},\mathbf{S},\mathbf{A},\mathbf{F},\mathbf{Q}) \in \mathbb{D}_4$, then by (4.9), we find

$$\begin{aligned}
\mathbb{L}\bar{\mathcal{H}} \quad &\leq \frac{-\varphi\mathbf{A}}{\mathbf{F}} + \mathcal{M}_1\\
&\leq \frac{-\varphi}{\epsilon} + \mathcal{M}_1.
\end{aligned}$$

If we choose a sufficiently small $\epsilon > 0$, then we get $\mathbb{L}\bar{\mathcal{H}} < 0$ for each $(\mathbf{U},\mathbf{S},\mathbf{A},\mathbf{F},\mathbf{Q}) \in \mathbb{D}_4$.

Case (e) If $(\mathbf{U},\mathbf{S},\mathbf{A},\mathbf{F},\mathbf{Q}) \in \mathbb{D}_5$, then by (4.9), we find

$$\begin{aligned}\mathbb{L}\bar{\mathcal{H}} &\leq -\mathcal{M}\mathbf{F} + (\mathcal{M}\ell_3 + 1)\xi\mathbf{Q} + \mathcal{N}_1\\ &\leq -\mathcal{M}\mathbf{F} + (\mathcal{M}\ell_3 + 1)\xi\epsilon + \mathcal{N}_1.\end{aligned}$$

If we choose a sufficiently small $\epsilon > 0$, then we get $\mathbb{L}\bar{\mathcal{H}} < 0$ for each $(\mathbf{U},\mathbf{S},\mathbf{A},\mathbf{F},\mathbf{Q}) \in \mathbb{D}_4$.
Case (f) If $(\mathbf{U},\mathbf{S},\mathbf{A},\mathbf{F},\mathbf{Q}) \in \mathbb{D}_6$, then by (4.9), we find

$$\begin{aligned}\mathbb{L}\bar{\mathcal{H}} &\leq -\frac{1}{4}\Big(c_1 - \frac{\theta}{2}(\rho_1^2 \vee \rho_2^2 \vee \rho_3^2 \vee \rho_4^2 \vee \rho_5^2)\Big)(\mathbf{U})^{\theta+1} + \mathcal{M}_1\\ &\leq -\frac{1}{4}\Big(c_1 - \frac{\theta}{2}(\rho_1^2 \vee \rho_2^2 \vee \rho_3^2 \vee \rho_4^2 \vee \rho_5^2)\Big)\frac{1}{\epsilon^{(\theta+1)}} + \mathcal{M}_1.\end{aligned}$$

If we choose a sufficiently small $\epsilon > 0$, then we get $\mathbb{L}\bar{\mathcal{H}} < 0$ for each $(\mathbf{U},\mathbf{S},\mathbf{A},\mathbf{F},\mathbf{Q}) \in \mathbb{D}_6$.
Case (g) If $(\mathbf{U},\mathbf{S},\mathbf{A},\mathbf{F},\mathbf{Q}) \in \mathbb{D}_7$, then by (4.9), we find

$$\begin{aligned}\mathbb{L}\bar{\mathcal{H}} &\leq -\frac{1}{4}\Big(c_1 - \frac{\theta}{2}(\rho_1^2 \vee \rho_2^2 \vee \rho_3^2 \vee \rho_4^2 \vee \rho_5^2)\Big)(\mathbf{S})^{\theta+1} + \mathcal{M}_1\\ &\leq -\frac{1}{4}\Big(c_1 - \frac{\theta}{2}(\rho_1^2 \vee \rho_2^2 \vee \rho_3^2 \vee \rho_4^2 \vee \rho_5^2)\Big)\frac{1}{\epsilon^{5(\theta+1)}} + \mathcal{M}_1.\end{aligned}$$

If we choose a sufficiently small $1/\epsilon^5 > 0$, then we get $\mathbb{L}\bar{\mathcal{H}} < 0$ for each $(\mathbf{U},\mathbf{S},\mathbf{A},\mathbf{F},\mathbf{Q}) \in \mathbb{D}_7$.
Case (h) If $(\mathbf{U},\mathbf{S},\mathbf{A},\mathbf{F},\mathbf{Q}) \in \mathbb{D}_8$, then by (4.9), we find

$$\begin{aligned}\mathbb{L}\bar{\mathcal{H}} &\leq -\frac{1}{4}\Big(c_1 - \frac{\theta}{2}(\rho_1^2 \vee \rho_2^2 \vee \rho_3^2 \vee \rho_4^2 \vee \rho_5^2)\Big)(\mathbf{A})^{\theta+1} + \mathcal{M}_1\\ &\leq -\frac{1}{4}\Big(c_1 - \frac{\theta}{2}(\rho_1^2 \vee \rho_2^2 \vee \rho_3^2 \vee \rho_4^2 \vee \rho_5^2)\Big)\frac{1}{\epsilon^{2(\theta+1)}} + \mathcal{M}_1.\end{aligned}$$

If we choose a sufficiently small $1/\epsilon^2 > 0$, then we get $\mathbb{L}\bar{\mathcal{H}} < 0$ for each $(\mathbf{U},\mathbf{S},\mathbf{A},\mathbf{F},\mathbf{Q}) \in \mathbb{D}_8$.
Case (i) If $(\mathbf{U},\mathbf{S},\mathbf{A},\mathbf{F},\mathbf{Q}) \in \mathbb{D}_9$, then by (4.9), we find

$$\begin{aligned}\mathbb{L}\bar{\mathcal{H}} &\leq -\frac{1}{4}\Big(c_1 - \frac{\theta}{2}(\rho_1^2 \vee \rho_2^2 \vee \rho_3^2 \vee \rho_4^2 \vee \rho_5^2)\Big)(\mathbf{F})^{\theta+1} + \mathcal{M}_1\\ &\leq -\frac{1}{4}\Big(c_1 - \frac{\theta}{2}(\rho_1^2 \vee \rho_2^2 \vee \rho_3^2 \vee \rho_4^2 \vee \rho_5^2)\Big)\frac{1}{\epsilon^{3(\theta+1)}} + \mathcal{M}_1.\end{aligned}$$

If we choose a sufficiently small $1/\epsilon^3 > 0$, then we get $\mathbb{L}\bar{\mathcal{H}} < 0$ for each $(\mathbf{U},\mathbf{S},\mathbf{A},\mathbf{F},\mathbf{Q}) \in \mathbb{D}_9$.
Case (j) If $(\mathbf{U},\mathbf{S},\mathbf{A},\mathbf{F},\mathbf{Q}) \in \mathbb{D}_{10}$, then by (4.9), we find

$$\begin{aligned}\mathbb{L}\bar{\mathcal{H}} &\leq -\frac{1}{4}\Big(c_1 - \frac{\theta}{2}(\rho_1^2 \vee \rho_2^2 \vee \rho_3^2 \vee \rho_4^2 \vee \rho_5^2)\Big)(\mathbf{Q})^{\theta+1} + \mathcal{M}_1\\ &\leq -\frac{1}{4}\Big(c_1 - \frac{\theta}{2}(\rho_1^2 \vee \rho_2^2 \vee \rho_3^2 \vee \rho_4^2 \vee \rho_5^2)\Big)\frac{1}{\epsilon^{(\theta+1)}} + \mathcal{M}_1.\end{aligned}$$

If we choose a sufficiently small $1/\epsilon > 0$, then we get $\mathbb{L}\bar{\mathcal{H}} < 0$ for each $(\mathbf{U},\mathbf{S},\mathbf{A},\mathbf{F},\mathbf{Q}) \in \mathbb{D}_{10}$.
As a result of the foregoing explanation, a $\epsilon > 0$ exists such that $\mathbb{L}\bar{\mathcal{H}}(\mathbf{U},\mathbf{S},\mathbf{A},\mathbf{F},\mathbf{Q}) < 0\ \forall\ (\mathbf{U},\mathbf{S},\mathbf{A},\mathbf{F},\mathbf{Q}) \in \mathbb{R}_+^5$. The unique ESD of the system (3.2) is predicated on Lemma 4.1. This completes the proof.

4.2. Extinction of the model

This part defines the objectives for a virus's systemic elimination (3.1). Before proving the key findings, let's take a closer look at a key premise. Suppose

$$\langle \Phi(\bar{\mathbf{t}}) \rangle = \frac{1}{\bar{\mathbf{t}}} \int_0^{\bar{\mathbf{t}}} \phi(r_1) dr_1. \tag{4.13}$$

Theorem 4.3. *Suppose there is a solution of the system* (3.1) $(\mathbf{U}(\bar{\mathbf{t}}), \mathbf{S}(\bar{\mathbf{t}}), \mathbf{A}(\bar{\mathbf{t}}), \mathbf{F}(\bar{\mathbf{t}}), \mathbf{Q}(\bar{\mathbf{t}}))$ *having ICs lies in* $\mathbb{R}^5_+$. *If*

$$\tilde{\mathbb{R}}_0^s := \frac{3(\lambda_1 + \lambda_2)\Lambda}{\varsigma((\nu_1 + \frac{\rho_2^2}{2}) \wedge ((\delta - \varphi) + \frac{\rho_3^2}{2}) \wedge (\nu_2 + \frac{\rho_4^2}{2}))} < 1$$

$$\Longrightarrow \lim_{\bar{\mathbf{t}} \mapsto \infty} \frac{1}{\bar{\mathbf{t}}} \int_0^{\bar{\mathbf{t}}} \mathbf{U}(\varpi) d\varpi \leq \frac{\Lambda}{\varsigma}, \ \lim_{\bar{\mathbf{t}} \mapsto \infty} \mathbf{S}(\bar{\mathbf{t}}) = 0, \ \lim_{\bar{\mathbf{t}} \mapsto \infty} \mathbf{A}(\bar{\mathbf{t}}) = 0, \ \lim_{\bar{\mathbf{t}} \mapsto \infty} \mathbf{F}(\bar{\mathbf{t}}) = 0$$

almost surely.

Proof. Under the hypothesis of Theorem 4.1, model (3.2) has non-negative solution,

$$d\mathbf{U}(\bar{\mathbf{t}}) \leq (\Lambda - \varsigma \mathbf{U}) d\bar{\mathbf{t}} + \rho_1 \mathbf{U} d\mathbf{B}_1(\bar{\mathbf{t}}).$$

Assume the stochastic DE of the aforementioned system

$$d\mathbf{U}_1(\bar{\mathbf{t}}) \leq (\Lambda - \varsigma \mathbf{U}_1) d\bar{\mathbf{t}} + \rho_1 \mathbf{U}_1 d\mathbf{B}_1(\bar{\mathbf{t}}), \ \ \mathbf{U}_1(0) = \mathbf{U}(0) > 0,$$

we have $\lim\limits_{\bar{\mathbf{t}} \mapsto \infty} \frac{1}{\bar{\mathbf{t}}} \int\limits_0^{\bar{\mathbf{t}}} \mathbf{U}(\varpi) d\varpi \leq \frac{\Lambda}{\varsigma}$ $(a.s)$.
Applying the result of [48], gives $\mathbf{U}(\bar{\mathbf{t}}) \leq \mathbf{U}_1(\bar{\mathbf{t}})$ $(a.s)$. Then

$$\lim_{\bar{\mathbf{t}} \mapsto \infty} \frac{1}{\bar{\mathbf{t}}} \int_0^{\bar{\mathbf{t}}} \mathbf{U}(\varpi) d\varpi \leq \lim_{\bar{\mathbf{t}} \mapsto \infty} \frac{1}{\bar{\mathbf{t}}} \int_0^{\bar{\mathbf{t}}} \mathbf{U}_1(\varpi) d\varpi = \frac{\Lambda}{\varsigma} \ (a.s).$$

For $\varphi < \delta$ and introducing $\ln(\mathbf{S}(\bar{\mathbf{t}}) + \mathbf{A}(\bar{\mathbf{t}}) + \mathbf{F}(\bar{\mathbf{t}}))$ and implement the Itô's technique, we have

$$\begin{aligned} d(\ln(\mathbf{S}(\bar{\mathbf{t}}) + \mathbf{A}(\bar{\mathbf{t}}) + \mathbf{F}(\bar{\mathbf{t}}))) \quad &= \frac{1}{\mathbf{S}(\bar{\mathbf{t}}) + \mathbf{A}(\bar{\mathbf{t}}) + \mathbf{F}(\bar{\mathbf{t}})} \Big(\frac{\lambda_1 \mathbf{U}\mathbf{F}}{1 + \mathbf{F}} + \frac{\lambda_2 \mathbf{U}\mathbf{A}}{1 + \mathbf{A}} - \nu_1 \mathbf{S} - (\delta - \varphi)\mathbf{A} \\ &\quad - \nu_2 \mathbf{F} - \xi \mathbf{F}\mathbf{Q} \Big) d\bar{\mathbf{t}} + \frac{\rho_2 \mathbf{S}}{\mathbf{S} + \mathbf{A} + \mathbf{F}} d\mathbf{B}_2(\bar{\mathbf{t}}) + \frac{\rho_3 \mathbf{A}}{\mathbf{S} + \mathbf{A} + \mathbf{F}} d\mathbf{B}_3(\bar{\mathbf{t}}) \\ &\quad + \frac{\rho_4 \mathbf{F}}{\mathbf{S} + \mathbf{A} + \mathbf{F}} d\mathbf{B}_2(\bar{\mathbf{t}}) - \frac{1}{2(\mathbf{S} + \mathbf{A} + \mathbf{F})^2} (\rho_2^2 \mathbf{S}^2 + \rho_3^2 \mathbf{A}^2 + \rho_4^2 \mathbf{F}^2) d\bar{\mathbf{t}} \\ &\leq \frac{\rho_2 \mathbf{S}}{\mathbf{S} + \mathbf{A} + \mathbf{F}} d\mathbf{B}_2(\bar{\mathbf{t}}) + \frac{\rho_3 \mathbf{A}}{\mathbf{S} + \mathbf{A} + \mathbf{F}} d\mathbf{B}_3(\bar{\mathbf{t}}) + \frac{\rho_4 \mathbf{F}}{\mathbf{S} + \mathbf{A} + \mathbf{F}} d\mathbf{B}_2(\bar{\mathbf{t}}) \\ &\quad + (\lambda_1 + \lambda_2) \mathbf{U} d\bar{\mathbf{t}} - \frac{1}{3} \Big(((\nu_1 + \frac{\rho_2^2}{2}) \wedge ((\delta - \varphi) + \frac{\rho_3^2}{2}) \wedge (\nu_2 + \frac{\rho_4^2}{2})) \Big) d\bar{\mathbf{t}}. \end{aligned} \tag{4.14}$$

Applying integration from 0 to $\bar{\mathbf{t}}$ and dividing by $\bar{\mathbf{t}}$, we have

$$\begin{aligned}
&\frac{\ln(\mathbf{S}(\bar{\mathbf{t}})+\mathbf{A}(\bar{\mathbf{t}})+\mathbf{F}(\bar{\mathbf{t}}))}{\bar{\mathbf{t}}} - \frac{\ln(\mathbf{S}(0)+\mathbf{A}(0)+\mathbf{F}(0))}{\bar{\mathbf{t}}}\\
&\leq \frac{\lambda_1+\lambda_2}{\bar{\mathbf{t}}}\int_0^{\bar{\mathbf{t}}}\mathbf{U}(\varrho)d\varrho - \frac{1}{3}\Big(((\nu_1+\frac{\rho_2^2}{2})\wedge((\delta-\varphi)+\frac{\rho_3^2}{2})\wedge(\nu_2+\frac{\rho_4^2}{2}))\Big)\\
&\quad+\frac{\rho_2}{\bar{\mathbf{t}}}\int_0^{\bar{\mathbf{t}}}\frac{d\mathbf{B}_2(\varrho)}{\mathbf{S}+\mathbf{A}+\mathbf{F}}+\frac{\rho_3}{\bar{\mathbf{t}}}\int_0^{\bar{\mathbf{t}}}\frac{d\mathbf{B}_3(\varrho)}{\mathbf{S}+\mathbf{A}+\mathbf{F}}+\frac{\rho_4}{\bar{\mathbf{t}}}\int_0^{\bar{\mathbf{t}}}\frac{d\mathbf{B}_4(\varrho)}{\mathbf{S}+\mathbf{A}+\mathbf{F}}\\
&\leq \frac{1}{3}\Big(((\nu_1+\frac{\rho_2^2}{2})\wedge((\delta-\varphi)+\frac{\rho_3^2}{2})\wedge(\nu_2+\frac{\rho_4^2}{2}))\Big)(\tilde{\mathbb{R}}_0^s-1)<0\ (a.s)
\end{aligned}$$

that yields $\lim_{\bar{\mathbf{t}}\mapsto\infty}\mathbf{S}(\bar{\mathbf{t}})=0,\ \lim_{\bar{\mathbf{t}}\mapsto\infty}\mathbf{A}(\bar{\mathbf{t}})=0,\ \lim_{\bar{\mathbf{t}}\mapsto\infty}\mathbf{F}(\bar{\mathbf{t}})\ (a.s)$.

5. Numerical experiment for fractal–fractional system

The modeling framework helps us understand and interpret experimental data on immune responses against viral infection model (5.1). The role of the fractal-fractional operator in the Atangana-Baleanu fractional derivative sense and antibodies for the resolution of viral infection is debated by utilizing the scheme proposed in [52]. Studies of the acute phase of the infection showed that humans who cleared the virus from their blood developed strong and sustained CTL responses [57]. Here, we illustrate the fractal-fractional derivative for the classical derivative formulation stated in (3.1). The fractal-fractional version in the sense of a generalized Mittag-Leffler function is described as

$$\begin{cases}
{}^{\mathbf{FFM}}_{0}\mathbf{D}^{\alpha,\wp}_{\bar{\mathbf{t}}}\mathbf{U}(\bar{\mathbf{t}}) = \Big(\Lambda-\varsigma\mathbf{U}(\bar{\mathbf{t}})-\frac{\lambda_1\mathbf{U}(\bar{\mathbf{t}})\mathbf{S}(\bar{\mathbf{t}})}{1+\mathbf{S}(\bar{\mathbf{t}})}-\frac{\lambda_2\mathbf{U}(\bar{\mathbf{t}})\mathbf{A}(\bar{\mathbf{t}})}{1+\mathbf{A}(t_1)}\Big)dt_1+\rho_1\mathcal{G}_1(t_1,\mathbf{U})d\mathbf{B}_1(\bar{\mathbf{t}}),\\
{}^{\mathbf{FFM}}_{0}\mathbf{D}^{\alpha,\wp}_{\bar{\mathbf{t}}}\mathbf{S}(\bar{\mathbf{t}}) = \Big((1-\phi)\Big(\frac{\lambda_1\mathbf{U}(\bar{\mathbf{t}})\mathbf{S}(\bar{\mathbf{t}})}{1+\mathbf{S}(\bar{\mathbf{t}})}+\frac{\lambda_2\mathbf{U}(\bar{\mathbf{t}})\mathbf{A}(\bar{\mathbf{t}})}{1+\mathbf{A}(\bar{\mathbf{t}})}\Big)-(\nu_1+\sigma)\mathbf{S}(\bar{\mathbf{t}})\Big)d\bar{\mathbf{t}}+\rho_2\mathcal{G}_2(\bar{\mathbf{t}},\mathbf{S})d\mathbf{B}_2(\bar{\mathbf{t}}),\\
{}^{\mathbf{FFM}}_{0}\mathbf{D}^{\alpha,\wp}_{\bar{\mathbf{t}}}\mathbf{A}(\bar{\mathbf{t}}) = \Big(\phi\Big(\frac{\lambda_1\mathbf{U}(\bar{\mathbf{t}})\mathbf{S}(\bar{\mathbf{t}})}{1+\mathbf{S}(\bar{\mathbf{t}})}+\frac{\lambda_2\mathbf{U}(\bar{\mathbf{t}})\mathbf{A}(\bar{\mathbf{t}})}{1+\mathbf{A}(\bar{\mathbf{t}})}\Big)+\sigma\mathbf{S}(\bar{\mathbf{t}})-\delta\mathbf{A}(\bar{\mathbf{t}})\Big)d\bar{\mathbf{t}}+\rho_3\mathcal{G}_3(\bar{\mathbf{t}},\mathbf{A})d\mathbf{B}_3(\bar{\mathbf{t}}),\\
{}^{\mathbf{FFM}}_{0}\mathbf{D}^{\alpha,\wp}_{\bar{\mathbf{t}}}\mathbf{F}(\bar{\mathbf{t}}) = \Big(\varphi\mathbf{A}(\bar{\mathbf{t}})-\nu_2\mathbf{F}(\bar{\mathbf{t}})-\xi\mathbf{F}(\bar{\mathbf{t}})\mathbf{Q}(\bar{\mathbf{t}})\Big)d\bar{\mathbf{t}}+\rho_4\mathcal{G}_4(\bar{\mathbf{t}},\mathbf{F})d\mathbf{B}_4(\bar{\mathbf{t}}),\\
{}^{\mathbf{FFM}}_{0}\mathbf{D}^{\alpha,\wp}_{\bar{\mathbf{t}}}\mathbf{Q}(\bar{\mathbf{t}}) = \Big(\chi\mathbf{F}(\bar{\mathbf{t}})\mathbf{Q}(\bar{\mathbf{t}})-\zeta\mathbf{Q}(\bar{\mathbf{t}})\Big)d\bar{\mathbf{t}}+\rho_5\mathcal{G}_5(\bar{\mathbf{t}},\mathbf{Q})d\mathbf{B}_5(\bar{\mathbf{t}}).
\end{cases}\tag{5.1}$$

For $t_{\mathfrak{n}+1}=(\mathfrak{n}+1)\Delta\bar{\mathbf{t}}$, then we transform these mappings by their polynomials as follows:

$$\begin{aligned}
\mathbf{U}_{\mathfrak{n}+1} &= \mathbf{U}_0+\frac{(1-\alpha)}{\mathbf{ABC}(\alpha)}\wp\bar{\mathbf{t}}^{\wp-1}_{\mathfrak{n}+1}\begin{bmatrix}\{\mathbf{U}^*(\bar{\mathbf{t}}_{\mathfrak{n}+1},\mathbf{U}^p_{\mathfrak{n}+1},\mathbf{A}^p_{\mathfrak{n}+1},\mathbf{F}^p_{\mathfrak{n}+1})\\ +\rho_1\mathcal{G}_1(\bar{\mathbf{t}}_{\mathfrak{n}+1},\mathbf{U}^p_{\mathfrak{n}+1})(\mathbf{B}_1(\bar{\mathbf{t}}_{\mathfrak{n}+2})-\mathbf{B}_1(\bar{\mathbf{t}}_{\mathfrak{n}+1}))\end{bmatrix}\\
&\quad+\frac{\alpha\wp}{\mathbf{ABC}(\alpha)\Gamma(\alpha)}\sum_{\kappa=0}^{\mathfrak{n}-1}\begin{bmatrix}\{\mathbf{U}^*(\bar{\mathbf{t}}_{\kappa+1},\mathbf{U}_{\kappa+1},\mathbf{A}_{\kappa+1},\mathbf{F}_{\kappa+1})\mathcal{J}^{\alpha,\wp}_{1,\kappa}\\ +\frac{\mathbf{U}^*(\bar{\mathbf{t}}_{\kappa+1},\mathbf{U}_{\kappa+1},\mathbf{A}_{\kappa+1},\mathbf{F}_{\kappa+1})-\mathbf{U}^*(\bar{\mathbf{t}}_{\kappa},\mathbf{U}_{\kappa},\mathbf{A}_{\kappa},\mathbf{F}_{\kappa})}{\hbar}\mathcal{J}^{\alpha,\wp}_{2,\kappa}\\ +\frac{\mathbf{U}^*(\bar{\mathbf{t}}_{\kappa+1},\mathbf{U}_{\kappa+1},\mathbf{A}_{\kappa+1},\mathbf{F}_{\kappa+1})-2\mathbf{U}^*(\bar{\mathbf{t}}_{\kappa},\mathbf{U}_{\kappa},\mathbf{A}_{\kappa},\mathbf{F}_{\kappa})+\mathbf{U}^*(\bar{\mathbf{t}}_{\kappa-1},\mathbf{U}_{\kappa-1},\mathbf{A}_{\kappa-1},\mathbf{F}_{\kappa-1})}{\hbar}\mathcal{J}^{\alpha,\wp}_{3,\kappa}\end{bmatrix}\\
&\quad+\frac{\alpha\wp}{\mathbf{ABC}(\alpha)\Gamma(\alpha)}\sum_{\kappa=0}^{\mathfrak{n}-1}\begin{bmatrix}\rho_1\mathcal{G}_1(\bar{\mathbf{t}}_{\kappa+1},\mathbf{U}_{\kappa+1})(\mathbf{B}_1(\bar{\mathbf{t}}_{\kappa+1})-\mathbf{B}_1(\bar{\mathbf{t}}_{\kappa}))\mathcal{J}^{\alpha,\wp}_{1,\kappa}\\ +\Big\{\rho_1\mathcal{G}_1(\bar{\mathbf{t}}_{\kappa+1},\mathbf{U}_{\kappa+1})(\mathbf{B}_1(\bar{\mathbf{t}}_{\kappa+1})-\mathbf{B}_1(\bar{\mathbf{t}}_{\kappa}))\\ -\rho_1\mathcal{G}_1(\bar{\mathbf{t}}_{\kappa},\mathbf{U}_{\kappa})(\mathbf{B}_1(\bar{\mathbf{t}}_{\kappa})-\mathbf{B}_1(\bar{\mathbf{t}}_{\kappa-1}))\Big\}\mathcal{J}^{\alpha,\wp}_{2,\kappa}\\ +\Big\{\frac{\rho_1\mathcal{G}_1(\bar{\mathbf{t}}_{\kappa+1},\mathbf{U}_{\kappa+1})(\mathbf{B}_1(\bar{\mathbf{t}}_{\kappa+1})-\mathbf{B}_1(\bar{\mathbf{t}}_{\kappa}))-2\rho_1\mathcal{G}_1(\bar{\mathbf{t}}_{\kappa},\mathbf{U}_{\kappa})(\mathbf{B}_1(\bar{\mathbf{t}}_{\kappa})-\mathbf{B}_1(\bar{\mathbf{t}}_{\kappa-1}))}{\hbar}\\ -\frac{\rho_1\mathcal{G}_1(\bar{\mathbf{t}}_{\kappa-1},\mathbf{U}_{\kappa-1})(\mathbf{B}_1(\bar{\mathbf{t}}_{\kappa-1})-\mathbf{B}_1(\bar{\mathbf{t}}_{\kappa-2}))}{\hbar}\Big\}\mathcal{J}^{\alpha,\wp}_{3,\kappa}\end{bmatrix}
\end{aligned}$$

$$+\frac{\alpha\wp}{\mathbf{ABC}(\alpha)\Gamma(\alpha)}\left[\begin{array}{l}\mathbf{U}^*(\bar{\mathbf{t}}_{n+1},\mathbf{U}^p_{n+1},\mathbf{A}^p_{n+1},\mathbf{F}^p_{n+1})\mathcal{J}^{\alpha,\wp}_{1,n}\\ +\mathbf{U}^*(\bar{\mathbf{t}}_{n+1},\mathbf{U}^p_{n+1},\mathbf{A}^p_{n+1},\mathbf{F}^p_{n+1})\mathcal{J}^{\alpha,\wp}_{2,n}\\ -\mathbf{U}^*(\bar{\mathbf{t}}_n,\mathbf{U}_n,\mathbf{A}_n,\mathbf{F}_n)\mathcal{J}^{\alpha,\wp}_{2,n}\\ +\left\{\frac{\mathbf{U}^*\left(\bar{\mathbf{t}}_{n+1},\mathbf{U}^p_{n+1},\mathbf{A}^p_{n+1},\mathbf{F}^p_{n+1}\right)-2\mathbf{U}^*\left(\bar{\mathbf{t}}_n,\mathbf{U}_n,\mathbf{A}_n,\mathbf{F}_n\right)}{2\hbar}\right\}\mathcal{J}^{\alpha,\wp}_{3,n}\\ +\frac{\mathbf{U}^*\left(\bar{\mathbf{t}}_{n-1},\mathbf{U}_{n-1},\mathbf{A}_{n-1},\mathbf{F}_{n-1}\right)}{2\hbar^2}\mathcal{J}^{\alpha,\wp}_{3,n}\\ +\rho_1\mathcal{G}_1(\bar{\mathbf{t}}_{n+1},\mathbf{U}^{p_1}_{n+1})(\mathbf{B}_1(\bar{\mathbf{t}}_{n+1})-\mathbf{B}_1(\bar{\mathbf{t}}_n))\mathcal{J}^{\alpha,\wp}_{1,n}\\ +\rho_1\mathcal{G}_1(\bar{\mathbf{t}}_{n+1},\mathbf{U}^{p_1}_{n+1})(\mathbf{B}_1(\bar{\mathbf{t}}_{n+1})-\mathbf{B}_1(\bar{\mathbf{t}}_n))\mathcal{J}^{\alpha,\wp}_{2,n}\\ -\rho_1\mathcal{G}_1(\bar{\mathbf{t}}_n,\mathbf{U}^{p_1}_n)(\mathbf{B}_1(\bar{\mathbf{t}}_n)-\mathbf{B}_1(\bar{\mathbf{t}}_{n-1}))\mathcal{J}^{\alpha,\wp}_{2,n}\\ +\frac{\rho_1\mathcal{G}_1\left(\bar{\mathbf{t}}_{n+1},\mathbf{U}^{p_1}_{n+1}\right)\left(\mathbf{B}_1(\bar{\mathbf{t}}_{n+1})-\mathbf{B}_1(\bar{\mathbf{t}}_n)\right)}{2\hbar}\mathcal{J}^{\alpha,\wp}_{3,n}\\ -2\frac{\rho_1\mathcal{G}_1\left(\bar{\mathbf{t}}_n,\mathbf{U}^{p_1}_n\right)\left(\mathbf{B}_1(\bar{\mathbf{t}}_n)-\mathbf{B}_1(\bar{\mathbf{t}}_{n-1})\right)}{2\hbar}\mathcal{J}^{\alpha,\wp}_{3,n}\\ +\frac{\rho_1\mathcal{G}_1\left(\bar{\mathbf{t}}_{n-1},\mathbf{U}^{p_1}_{n-1}\right)\left(\mathbf{B}_1(\bar{\mathbf{t}}_{n-2})-\mathbf{B}_1(\bar{\mathbf{t}}_{n-2})\right)}{2\hbar}\mathcal{J}^{\alpha,\wp}_{3,n}\end{array}\right],$$

$$\begin{aligned}\mathbf{S}_{n+1} &= \mathbf{S}_0+\frac{(1-\alpha)}{\mathbf{ABC}(\alpha)}\wp\bar{\mathbf{t}}^{\wp-1}_{n+1}\left[\begin{array}{l}\mathbf{S}^*(\bar{\mathbf{t}}_{n+1},\mathbf{U}^p_{n+1},\mathbf{S}^p_{n+1},\mathbf{A}^p_{n+1},\mathbf{F}^p_{n+1})\\ +\rho_2\mathcal{G}_2(\bar{\mathbf{t}}_{n+1},\mathbf{S}^p_{n+1})(\mathbf{B}_2(\bar{\mathbf{t}}_{n+2})-\mathbf{B}_2(\bar{\mathbf{t}}_{n+1}))\end{array}\right]\\ &+\frac{\alpha\wp}{\mathbf{ABC}(\alpha)\Gamma(\alpha)}\sum_{\kappa=0}^{n-1}\left[\begin{array}{l}\mathbf{S}^*(\bar{\mathbf{t}}_{\kappa+1},\mathbf{U}_{\kappa+1},\mathbf{S}_{\kappa+1},\mathbf{A}_{\kappa+1},\mathbf{F}_{\kappa+1})\mathcal{J}^{\alpha,\wp}_{1,\kappa}\\ +\frac{\mathbf{S}^*\left(\bar{\mathbf{t}}_{\kappa+1},\mathbf{U}_{\kappa+1},\mathbf{S}_{\kappa+1},\mathbf{A}_{\kappa+1},\mathbf{F}_{\kappa+1}\right)-\mathbf{S}^*\left(\bar{\mathbf{t}}_\kappa,\mathbf{U}_\kappa,\mathbf{S}_\kappa,\mathbf{A}_\kappa,\mathbf{F}_\kappa\right)}{\hbar}\mathcal{J}^{\alpha,\wp}_{2,\kappa}\\ +\left(\frac{\mathbf{S}^*\left(\bar{\mathbf{t}}_{\kappa+1},\mathbf{U}_{\kappa+1},\mathbf{S}_{\kappa+1},\mathbf{A}_{\kappa+1},\mathbf{F}_{\kappa+1}\right)-2\mathbf{S}^*\left(\bar{\mathbf{t}}_\kappa,\mathbf{U}_\kappa,\mathbf{S}_\kappa,\mathbf{A}_\kappa,\mathbf{F}_\kappa\right)}{\hbar}\right.\\ \left.+\frac{\mathbf{S}^*\left(\bar{\mathbf{t}}_{\kappa-1},\mathbf{U}_{\kappa-1},\mathbf{S}_{\kappa-1},\mathbf{A}_{\kappa-1},\mathbf{F}_{\kappa-1}\right)}{\hbar}\right)\mathcal{J}^{\alpha,\wp}_{3,\kappa}\end{array}\right]\\ &+\frac{\alpha\wp}{\mathbf{ABC}(\alpha)\Gamma(\alpha)}\sum_{\kappa=0}^{n-1}\left[\begin{array}{l}\rho_2\mathcal{G}_2(\bar{\mathbf{t}}_{\kappa+1},\mathbf{S}_{\kappa+1})(\mathbf{B}_2(\bar{\mathbf{t}}_{\kappa+1})-\mathbf{B}_2(\bar{\mathbf{t}}_\kappa))\mathcal{J}^{\alpha,\wp}_{1,\kappa}\\ +\left\{\rho_2\mathcal{G}_2(\bar{\mathbf{t}}_{\kappa+1},\mathbf{S}_{\kappa+1})(\mathbf{B}_2(\bar{\mathbf{t}}_{\kappa+1})-\mathbf{B}_2(\bar{\mathbf{t}}_\kappa))\right.\\ \left.-\rho_2\mathcal{G}_2(\bar{\mathbf{t}}_\kappa,\mathbf{S}_\kappa)(\mathbf{B}_2(\bar{\mathbf{t}}_\kappa)-\mathbf{B}_2(\bar{\mathbf{t}}_{\kappa-1}))\right\}\mathcal{J}^{\alpha,\wp}_{2,\kappa}\\ +\left\{\frac{\rho_2\mathcal{G}_2\left(\bar{\mathbf{t}}_{\kappa+1},\mathbf{S}_{\kappa+1}\right)\left(\mathbf{B}_2(\bar{\mathbf{t}}_{\kappa+1})-\mathbf{B}_2(\bar{\mathbf{t}}_\kappa)\right)-2\rho_2\mathcal{G}_2\left(\bar{\mathbf{t}}_\kappa,\mathbf{S}_\kappa\right)\left(\mathbf{B}_2(\bar{\mathbf{t}}_\kappa)-\mathbf{B}_2(\bar{\mathbf{t}}_{\kappa-1})\right)}{\hbar}\right.\\ \left.-\frac{\rho_2\mathcal{G}_2\left(\bar{\mathbf{t}}_{\kappa-1},\mathbf{S}_{\kappa-1}\right)\left(\mathbf{B}_2(\bar{\mathbf{t}}_{\kappa-1})-\mathbf{B}_2(\bar{\mathbf{t}}_{\kappa-2})\right)}{\hbar}\right\}\mathcal{J}^{\alpha,\wp}_{3,\kappa}\end{array}\right]\\ &+\frac{\alpha\wp}{\mathbf{ABC}(\alpha)\Gamma(\alpha)}\left[\begin{array}{l}\mathbf{S}^*(\bar{\mathbf{t}}_{n+1},\mathbf{U}^p_{n+1},\mathbf{S}^p_{n+1},\mathbf{A}^p_{n+1},\mathbf{F}^p_{n+1})\mathcal{J}^{\alpha,\wp}_{1,n}\\ +\mathbf{S}^*(\bar{\mathbf{t}}_{n+1},\mathbf{U}^p_{n+1},\mathbf{S}^p_{n+1},\mathbf{A}^p_{n+1},\mathbf{F}^p_{n+1})\mathcal{J}^{\alpha,\wp}_{2,n}\\ -\mathbf{S}^*(\bar{\mathbf{t}}_n,\mathbf{U}_n,\mathbf{S}_n,\mathbf{A}_n,\mathbf{F}_n)\mathcal{J}^{\alpha,\wp}_{2,n}\\ +\left\{\frac{\mathbf{S}^*\left(\bar{\mathbf{t}}_{n+1},\mathbf{U}^p_{n+1},\mathbf{S}^p_{n+1},\mathbf{A}^p_{n+1},\mathbf{F}^p_{n+1}\right)-2\mathbf{S}^*\left(\bar{\mathbf{t}}_n,\mathbf{U}_n,\mathbf{S}_n,\mathbf{A}_n,\mathbf{F}_n\right)}{2\hbar}\right\}\mathcal{J}^{\alpha,\wp}_{3,n}\\ +\frac{\mathbf{S}^*\left(\bar{\mathbf{t}}_{n-1},\mathbf{U}_{n-1},\mathbf{S}_{n-1},\mathbf{A}_{n-1},\mathbf{F}_{n-1}\right)}{2\hbar^2}\mathcal{J}^{\alpha,\wp}_{3,n}\\ +\rho_2\mathcal{G}_2(\bar{\mathbf{t}}_{n+1},\mathbf{S}^{p_1}_{n+1})(\mathbf{B}_2(\bar{\mathbf{t}}_{n+1})-\mathbf{B}_2(\bar{\mathbf{t}}_n))\mathcal{J}^{\alpha,\wp}_{1,n}\\ +\rho_2\mathcal{G}_2(\bar{\mathbf{t}}_{n+1},\mathbf{S}^{p_1}_{n+1})(\mathbf{B}_2(\bar{\mathbf{t}}_{n+1})-\mathbf{B}_2(\bar{\mathbf{t}}_n))\mathcal{J}^{\alpha,\wp}_{2,n}\\ -\rho_2\mathcal{G}_2(\bar{\mathbf{t}}_n,\mathbf{S}^{p_1}_n)(\mathbf{B}_2(\bar{\mathbf{t}}_n)-\mathbf{B}_2(\bar{\mathbf{t}}_{n-1}))\mathcal{J}^{\alpha,\wp}_{2,n}\\ +\frac{\rho_2\mathcal{G}_2\left(\bar{\mathbf{t}}_{n+1},\mathbf{S}^{p_1}_{n+1}\right)\left(\mathbf{B}_2(\bar{\mathbf{t}}_{n+1})-\mathbf{B}_2(\bar{\mathbf{t}}_n)\right)}{2\hbar}\mathcal{J}^{\alpha,\wp}_{3,n}\\ -2\frac{\rho_2\mathcal{G}_2\left(\bar{\mathbf{t}}_n,\mathbf{S}^{p_1}_n\right)\left(\mathbf{B}_2(\bar{\mathbf{t}}_n)-\mathbf{B}_2(\bar{\mathbf{t}}_{n-1})\right)}{2\hbar}\mathcal{J}^{\alpha,\wp}_{3,n}\\ +\frac{\rho_2\mathcal{G}_2\left(\bar{\mathbf{t}}_{n-1},\mathbf{S}^{p_1}_{n-1}\right)\left(\mathbf{B}_2(\bar{\mathbf{t}}_{n-2})-\mathbf{B}_2(\bar{\mathbf{t}}_{n-2})\right)}{2\hbar}\mathcal{J}^{\alpha,\wp}_{3,n}\end{array}\right],\end{aligned}$$

$$
\begin{aligned}
\mathbf{A}_{n+1} &= \mathbf{A}_0 + \frac{(1-\alpha)}{\mathbf{ABC}(\alpha)}\wp\bar{\mathbf{t}}_{n+1}^{\wp-1}\left[\begin{Bmatrix}\mathbf{A}^*(\bar{\mathbf{t}}_{n+1},\mathbf{U}_{n+1}^p,\mathbf{S}_{n+1}^p,\mathbf{A}_{n+1}^p,\mathbf{F}_{n+1}^p)\\ +\rho_3\mathcal{G}_4(\bar{\mathbf{t}}_{n+1},\mathbf{A}_{n+1}^p)(\mathbf{B}_3(\bar{\mathbf{t}}_{n+2})-\mathbf{B}_3(\bar{\mathbf{t}}_{n+1}))\end{Bmatrix}\right]\\
&+\frac{\alpha\wp}{\mathbf{ABC}(\alpha)\Gamma(\alpha)}\sum_{\kappa=0}^{n-1}\left[\begin{Bmatrix}\mathbf{A}^*(\bar{\mathbf{t}}_{\kappa+1},\mathbf{U}_{\kappa+1},\mathbf{S}_{\kappa+1},\mathbf{A}_{\kappa+1},\mathbf{F}_{\kappa+1})\mathcal{J}_{1,\kappa}^{\alpha,\wp}\\ +\frac{\mathbf{A}^*\left(\bar{\mathbf{t}}_{\kappa+1},\mathbf{U}_{\kappa+1},\mathbf{S}_{\kappa+1},\mathbf{A}_{\kappa+1},\mathbf{F}_{\kappa+1}\right)-\mathbf{A}^*\left(\bar{\mathbf{t}}_{\kappa},\mathbf{U}_{\kappa},\mathbf{S}_{\kappa},\mathbf{A}_{\kappa},\mathbf{F}_{\kappa}\right)}{\hbar}\mathcal{J}_{2,\kappa}^{\alpha,\wp}\\ +\left(\frac{\mathbf{A}^*\left(\bar{\mathbf{t}}_{\kappa+1},\mathbf{U}_{\kappa+1},\mathbf{S}_{\kappa+1},\mathbf{A}_{\kappa+1},\mathbf{F}_{\kappa+1}\right)-2\mathbf{A}^*\left(\bar{\mathbf{t}}_{\kappa},\mathbf{U}_{\kappa},\mathbf{S}_{\kappa},\mathbf{A}_{\kappa},\mathbf{F}_{\kappa}\right)}{\hbar}\right.\\ \left.+\frac{\mathbf{A}^*\left(\bar{\mathbf{t}}_{\kappa-1},\mathbf{U}_{\kappa-1},\mathbf{S}_{\kappa-1},\mathbf{A}_{\kappa-1},\mathbf{F}_{\kappa-1}\right)}{\hbar}\right)\mathcal{J}_{3,\kappa}^{\alpha,\wp}\end{Bmatrix}\right]\\
&+\frac{\alpha\wp}{\mathbf{ABC}(\alpha)\Gamma(\alpha)}\sum_{\kappa=0}^{n-1}\left[\begin{Bmatrix}\rho_3\mathcal{G}_3(\bar{\mathbf{t}}_{\kappa+1},\mathbf{A}_{\kappa+1})(\mathbf{B}_3(\bar{\mathbf{t}}_{\kappa+1})-\mathbf{B}_3(\bar{\mathbf{t}}_{\kappa}))\mathcal{J}_{1,\kappa}^{\alpha,\wp}\\ +\left\{\rho_3\mathcal{G}_3(\bar{\mathbf{t}}_{\kappa+1},\mathbf{A}_{\kappa+1})(\mathbf{B}_3(\bar{\mathbf{t}}_{\kappa+1})-\mathbf{B}_3(\bar{\mathbf{t}}_{\kappa}))\right.\\ \left.-\rho_3\mathcal{G}_3(\bar{\mathbf{t}}_{\kappa},\mathbf{A}_{\kappa})(\mathbf{B}_3(\bar{\mathbf{t}}_{\kappa})-\mathbf{B}_3(\bar{\mathbf{t}}_{\kappa-1}))\right\}\mathcal{J}_{2,\kappa}^{\alpha,\wp}\\ +\left\{\frac{\rho_3\mathcal{G}_3\left(\bar{\mathbf{t}}_{\kappa+1},\mathbf{A}_{\kappa+1}\right)\left(\mathbf{B}_3(\bar{\mathbf{t}}_{\kappa+1})-\mathbf{B}_3(\bar{\mathbf{t}}_{\kappa})\right)-2\rho_3\mathcal{G}_3\left(\bar{\mathbf{t}}_{\kappa},\mathbf{A}_{\kappa}\right)\left(\mathbf{B}_3(\bar{\mathbf{t}}_{\kappa})-\mathbf{B}_3(\bar{\mathbf{t}}_{\kappa-1})\right)}{\hbar}\right.\\ \left.-\frac{\rho_3\mathcal{G}_3\left(\bar{\mathbf{t}}_{\kappa-1},\mathbf{A}_{\kappa-1}\right)\left(\mathbf{B}_3(\bar{\mathbf{t}}_{\kappa-1})-\mathbf{B}_3(\bar{\mathbf{t}}_{\kappa-2})\right)}{\hbar}\right\}\mathcal{J}_{3,\kappa}^{\alpha,\wp}\end{Bmatrix}\right]\\
&+\frac{\alpha\wp}{\mathbf{ABC}(\alpha)\Gamma(\alpha)}\left[\begin{Bmatrix}\mathbf{A}^*(\bar{\mathbf{t}}_{n+1},\mathbf{U}_{n+1}^p,\mathbf{S}_{n+1}^p,\mathbf{A}_{n+1}^p,\mathbf{F}_{n+1}^p)\mathcal{J}_{1,n}^{\alpha,\wp}\\ +\mathbf{A}^*(\bar{\mathbf{t}}_{n+1},\mathbf{U}_{n+1}^p,\mathbf{S}_{n+1}^p,\mathbf{A}_{n+1}^p,\mathbf{F}_{n+1}^p)\mathcal{J}_{2,n}^{\alpha,\wp}\\ -\mathbf{A}^*(\bar{\mathbf{t}}_{n},\mathbf{U}_{n},\mathbf{S}_{n},\mathbf{A}_{n},\mathbf{F}_{n})\mathcal{J}_{2,n}^{\alpha,\wp}\\ +\left\{\frac{\mathbf{A}^*\left(\bar{\mathbf{t}}_{n+1},\mathbf{U}_{n+1}^p,\mathbf{S}_{n+1}^p,\mathbf{A}_{n+1}^p,\mathbf{F}_{n+1}^p\right)-2\mathbf{A}^*\left(\bar{\mathbf{t}}_{n},\mathbf{U}_{n},\mathbf{S}_{n},\mathbf{A}_{n},\mathbf{F}_{n}\right)}{2\hbar}\right\}\mathcal{J}_{3,n}^{\alpha,\wp}\\ +\frac{\mathbf{A}^*\left(\bar{\mathbf{t}}_{n-1},\mathbf{U}_{n-1},\mathbf{A}_{n-1},\mathbf{F}_{n-1}\right)}{2\hbar^2}\mathcal{J}_{3,n}^{\alpha,\wp}\\ +\rho_3\mathcal{G}_3(\bar{\mathbf{t}}_{n+1},\mathbf{A}_{n+1}^{p_1})(\mathbf{B}_3(\bar{\mathbf{t}}_{n+1})-\mathbf{B}_3(\bar{\mathbf{t}}_{n}))\mathcal{J}_{1,n}^{\alpha,\wp}\\ +\rho_3\mathcal{G}_3(\bar{\mathbf{t}}_{n+1},\mathbf{A}_{n+1}^{p_1})(\mathbf{B}_3(\bar{\mathbf{t}}_{n+1})-\mathbf{B}_3(\bar{\mathbf{t}}_{n}))\mathcal{J}_{2,n}^{\alpha,\wp}\\ -\rho_3\mathcal{G}_3(\bar{\mathbf{t}}_{n},\mathbf{A}_{n}^{p_1})(\mathbf{B}_3(\bar{\mathbf{t}}_{n})-\mathbf{B}_3(\bar{\mathbf{t}}_{n-1}))\mathcal{J}_{2,n}^{\alpha,\wp}\\ +\frac{\rho_3\mathcal{G}_3\left(\bar{\mathbf{t}}_{n+1},\mathbf{A}_{n+1}^{p_1}\right)\left(\mathbf{B}_3(\bar{\mathbf{t}}_{n+1})-\mathbf{B}_3(\bar{\mathbf{t}}_{n})\right)}{2\hbar}\mathcal{J}_{3,n}^{\alpha,\wp}\\ -2\frac{\rho_3\mathcal{G}_3\left(\bar{\mathbf{t}}_{n},\mathbf{A}_{n}^{p_1}\right)\left(\mathbf{B}_3(\bar{\mathbf{t}}_{n})-\mathbf{B}_3(\bar{\mathbf{t}}_{n-1})\right)}{2\hbar}\mathcal{J}_{3,n}^{\alpha,\wp}\\ +\frac{\rho_3\mathcal{G}_3\left(\bar{\mathbf{t}}_{n-1},\mathbf{A}_{n-1}^{p_1}\right)\left(\mathbf{B}_3(\bar{\mathbf{t}}_{n-2})-\mathbf{B}_3(\bar{\mathbf{t}}_{n-2})\right)}{2\hbar}\mathcal{J}_{3,n}^{\alpha,\wp}\end{Bmatrix}\right],
\end{aligned}
$$

$$
\begin{aligned}
\mathbf{F}_{n+1} &= \mathbf{F}_0 + \frac{(1-\alpha)}{\mathbf{ABC}(\alpha)}\wp\bar{\mathbf{t}}_{n+1}^{\wp-1}\left[\begin{Bmatrix}\mathbf{F}^*(\bar{\mathbf{t}}_{n+1},\mathbf{A}_{n+1}^p,\mathbf{F}_{n+1}^p,\mathbf{Q}_{n+1}^p)\\ +\rho_4\mathcal{G}_4(\bar{\mathbf{t}}_{n+1},\mathbf{F}_{n+1}^p)(\mathbf{B}_4(\bar{\mathbf{t}}_{n+2})-\mathbf{B}_4(\bar{\mathbf{t}}_{n+1}))\end{Bmatrix}\right]\\
&+\frac{\alpha\wp}{\mathbf{ABC}(\alpha)\Gamma(\alpha)}\sum_{\kappa=0}^{n-1}\left[\begin{Bmatrix}\mathbf{F}^*(\bar{\mathbf{t}}_{\kappa+1},\mathbf{A}_{\kappa+1},\mathbf{F}_{\kappa+1},\mathbf{Q}_{\kappa+1})\mathcal{J}_{1,\kappa}^{\alpha,\wp}\\ +\frac{\mathbf{F}^*\left(\bar{\mathbf{t}}_{\kappa+1},\mathbf{A}_{\kappa+1},\mathbf{F}_{\kappa+1},\mathbf{Q}_{\kappa+1}\right)-\mathbf{F}^*\left(\bar{\mathbf{t}}_{\kappa},\mathbf{A}_{\kappa},\mathbf{F}_{\kappa},\mathbf{Q}_{\kappa}\right)}{\hbar}\mathcal{J}_{2,\kappa}^{\alpha,\wp}\\ +\frac{\mathbf{F}^*\left(\bar{\mathbf{t}}_{\kappa+1},\mathbf{A}_{\kappa+1},\mathbf{F}_{\kappa+1},\mathbf{Q}_{\kappa+1}\right)-2\mathbf{A}^*\left(\bar{\mathbf{t}}_{\kappa},\mathbf{A}_{\kappa},\mathbf{F}_{\kappa},\mathbf{Q}_{\kappa}\right)+\mathbf{F}^*\left(\bar{\mathbf{t}}_{\kappa-1},\mathbf{A}_{\kappa-1},\mathbf{F}_{\kappa-1},\mathbf{Q}_{\kappa-1}\right)}{\hbar}\mathcal{J}_{3,\kappa}^{\alpha,\wp}\end{Bmatrix}\right]
\end{aligned}
$$

$$+\frac{\alpha\varphi}{\mathbf{ABC}(\alpha)\Gamma(\alpha)}\sum_{\kappa=0}^{\mathfrak{n}-1}\left[\begin{array}{l}\Big\{\rho_4\mathcal{G}_4(\bar{\mathbf{t}}_{\kappa+1},\mathbf{F}_{\kappa+1})(\mathbf{B}_4(\bar{\mathbf{t}}_{\kappa+1})-\mathbf{B}_4(\bar{\mathbf{t}}_{\kappa}))\mathcal{J}_{1,\kappa}^{\alpha,\varphi}\\ +\Big\{\rho_4\mathcal{G}_4(\bar{\mathbf{t}}_{\kappa+1},\mathbf{F}_{\kappa+1})(\mathbf{B}_4(\bar{\mathbf{t}}_{\kappa+1})-\mathbf{B}_4(\bar{\mathbf{t}}_{\kappa}))\\ -\rho_4\mathcal{G}_4(\bar{\mathbf{t}}_{\kappa},\mathbf{F}_{\kappa})(\mathbf{B}_4(\bar{\mathbf{t}}_{\kappa})-\mathbf{B}_4(\bar{\mathbf{t}}_{\kappa-1}))\Big\}\mathcal{J}_{2,\kappa}^{\alpha,\varphi}\\ +\Big\{\frac{\rho_4\mathcal{G}_4\left(\bar{\mathbf{t}}_{\kappa+1},\mathbf{F}_{\kappa+1}\right)\left(\mathbf{B}_4(\bar{\mathbf{t}}_{\kappa+1})-\mathbf{B}_4(\bar{\mathbf{t}}_{\kappa})\right)-2\rho_4\mathcal{G}_4\left(\bar{\mathbf{t}}_{\kappa},\mathbf{F}_{\kappa}\right)\left(\mathbf{B}_4(\bar{\mathbf{t}}_{\kappa})-\mathbf{B}_4(\bar{\mathbf{t}}_{\kappa-1})\right)}{\hbar}\\ -\frac{\rho_4\mathcal{G}_4\left(\bar{\mathbf{t}}_{\kappa-1},\mathbf{F}_{\kappa-1}\right)\left(\mathbf{B}_4(\bar{\mathbf{t}}_{\kappa-1})-\mathbf{B}_4(\bar{\mathbf{t}}_{\kappa-2})\right)}{\hbar}\Big\}\mathcal{J}_{3,\kappa}^{\alpha,\varphi}\end{array}\right]$$

$$+\frac{\alpha\varphi}{\mathbf{ABC}(\alpha)\Gamma(\alpha)}\left[\begin{array}{l}\mathbf{F}^*(\bar{\mathbf{t}}_{\mathfrak{n}+1},\mathbf{A}_{\mathfrak{n}+1}^p,\mathbf{F}_{\mathfrak{n}+1}^p,\mathbf{Q}_{\mathfrak{n}+1}^p)\mathcal{J}_{1,\mathfrak{n}}^{\alpha,\varphi}\\ +\mathbf{F}^*(\bar{\mathbf{t}}_{\mathfrak{n}+1},\mathbf{A}_{\mathfrak{n}+1}^p,\mathbf{F}_{\mathfrak{n}+1}^p,\mathbf{Q}_{\mathfrak{n}+1}^p)\mathcal{J}_{2,\mathfrak{n}}^{\alpha,\varphi}\\ -\mathbf{F}^*(\bar{\mathbf{t}}_{\mathfrak{n}},\mathbf{A}_{\mathfrak{n}},\mathbf{F}_{\mathfrak{n}},\mathbf{Q}_{\mathfrak{n}})\mathcal{J}_{2,\mathfrak{n}}^{\alpha,\varphi}\\ +\Big\{\frac{\mathbf{F}^*\left(\bar{\mathbf{t}}_{\mathfrak{n}+1},\mathbf{A}_{\mathfrak{n}+1}^p,\mathbf{F}_{\mathfrak{n}+1}^p,\mathbf{Q}_{\mathfrak{n}+1}^p\right)-2\mathbf{F}^*\left(\bar{\mathbf{t}}_{\mathfrak{n}},\mathbf{A}_{\mathfrak{n}},\mathbf{F}_{\mathfrak{n}},\mathbf{Q}_{\mathfrak{n}}\right)}{2\hbar}\Big\}\mathcal{J}_{3,\mathfrak{n}}^{\alpha,\varphi}\\ +\frac{\mathbf{F}^*\left(\bar{\mathbf{t}}_{\mathfrak{n}-1},\mathbf{A}_{\mathfrak{n}-1},\mathbf{F}_{\mathfrak{n}-1},\mathbf{Q}_{\mathfrak{n}-1}\right)}{2\hbar^2}\mathcal{J}_{3,\mathfrak{n}}^{\alpha,\varphi}\\ +\rho_4\mathcal{G}_4(\bar{\mathbf{t}}_{\mathfrak{n}+1},\mathbf{F}_{\mathfrak{n}+1}^{p_1})(\mathbf{B}_4(\bar{\mathbf{t}}_{\mathfrak{n}+1})-\mathbf{B}_4(\bar{\mathbf{t}}_{\mathfrak{n}}))\mathcal{J}_{1,\mathfrak{n}}^{\alpha,\varphi}\\ +\rho_4\mathcal{G}_4(\bar{\mathbf{t}}_{\mathfrak{n}+1},\mathbf{F}_{\mathfrak{n}+1}^{p_1})(\mathbf{B}_4(\bar{\mathbf{t}}_{\mathfrak{n}+1})-\mathbf{B}_4(\bar{\mathbf{t}}_{\mathfrak{n}}))\mathcal{J}_{2,\mathfrak{n}}^{\alpha,\varphi}\\ -\rho_4\mathcal{G}_4(\bar{\mathbf{t}}_{\mathfrak{n}},\mathbf{F}_{\mathfrak{n}}^{p_1})(\mathbf{B}_4(\bar{\mathbf{t}}_{\mathfrak{n}})-\mathbf{B}_4(\bar{\mathbf{t}}_{\mathfrak{n}-1}))\mathcal{J}_{2,\mathfrak{n}}^{\alpha,\varphi}\\ +\frac{\rho_4\mathcal{G}_4\left(\bar{\mathbf{t}}_{\mathfrak{n}+1},\mathbf{F}_{\mathfrak{n}+1}^{p_1}\right)\left(\mathbf{B}_4(\bar{\mathbf{t}}_{\mathfrak{n}+1})-\mathbf{B}_4(\bar{\mathbf{t}}_{\mathfrak{n}})\right)}{2\hbar}\mathcal{J}_{3,\mathfrak{n}}^{\alpha,\varphi}\\ -2\frac{\rho_4\mathcal{G}_4\left(\bar{\mathbf{t}}_{\mathfrak{n}},\mathbf{F}_{\mathfrak{n}}^{p_1}\right)\left(\mathbf{B}_4(\bar{\mathbf{t}}_{\mathfrak{n}})-\mathbf{B}_4(\bar{\mathbf{t}}_{\mathfrak{n}-1})\right)}{2\hbar}\mathcal{J}_{3,\mathfrak{n}}^{\alpha,\varphi}\\ +\frac{\rho_4\mathcal{G}_4\left(\bar{\mathbf{t}}_{\mathfrak{n}-1},\mathbf{F}_{\mathfrak{n}-1}^{p_1}\right)\left(\mathbf{B}_4(\bar{\mathbf{t}}_{\mathfrak{n}-2})-\mathbf{B}_4(\bar{\mathbf{t}}_{\mathfrak{n}-2})\right)}{2\hbar}\mathcal{J}_{3,\mathfrak{n}}^{\alpha,\varphi}\end{array}\right],$$

$$\begin{aligned}\mathbf{Q}_{\mathfrak{n}+1} &= \mathbf{Q}_0+\frac{(1-\alpha)}{\mathbf{ABC}(\alpha)}\varphi\bar{\mathbf{t}}_{\mathfrak{n}+1}^{\varphi-1}\left[\begin{array}{l}\Big\{\mathbf{Q}^*(\bar{\mathbf{t}}_{\mathfrak{n}+1},\mathbf{F}_{\mathfrak{n}+1}^p,\mathbf{Q}_{\mathfrak{n}+1}^p)\\ +\rho_5\mathcal{G}_5(\bar{\mathbf{t}}_{\mathfrak{n}+1},\mathbf{Q}_{\mathfrak{n}+1}^p)(\mathbf{B}_5(\bar{\mathbf{t}}_{\mathfrak{n}+2})-\mathbf{B}_5(\bar{\mathbf{t}}_{\mathfrak{n}+1}))\end{array}\right]\\ &+\frac{\alpha\varphi}{\mathbf{ABC}(\alpha)\Gamma(\alpha)}\sum_{\kappa=0}^{\mathfrak{n}-1}\left[\begin{array}{l}\Big\{\mathbf{Q}^*(\bar{\mathbf{t}}_{\kappa+1},\mathbf{F}_{\kappa+1},\mathbf{Q}_{\kappa+1})\mathcal{J}_{1,\kappa}^{\alpha,\varphi}\\ +\frac{\mathbf{Q}^*\left(\bar{\mathbf{t}}_{\kappa+1},\mathbf{F}_{\kappa+1},\mathbf{Q}_{\kappa+1}\right)-\mathbf{Q}^*\left(\bar{\mathbf{t}}_{\kappa},\mathbf{F}_{\kappa},\mathbf{Q}_{\kappa}\right)}{\hbar}\mathcal{J}_{2,\kappa}^{\alpha,\varphi}\\ +\frac{\mathbf{Q}^*\left(\bar{\mathbf{t}}_{\kappa+1},\mathbf{F}_{\kappa+1},\mathbf{Q}_{\kappa+1}\right)-2\mathbf{Q}^*\left(\bar{\mathbf{t}}_{\kappa},\mathbf{F}_{\kappa},\mathbf{Q}_{\kappa}\right)+\mathbf{Q}^*\left(\bar{\mathbf{t}}_{\kappa-1},\mathbf{F}_{\kappa-1},\mathbf{Q}_{\kappa-1}\right)}{\hbar}\mathcal{J}_{3,\kappa}^{\alpha,\varphi}\end{array}\right]\\ &+\frac{\alpha\varphi}{\mathbf{ABC}(\alpha)\Gamma(\alpha)}\sum_{\kappa=0}^{\mathfrak{n}-1}\left[\begin{array}{l}\Big\{\rho_5\mathcal{G}_5(\bar{\mathbf{t}}_{\kappa+1},\mathbf{Q}_{\kappa+1})(\mathbf{B}_5(\bar{\mathbf{t}}_{\kappa+1})-\mathbf{B}_5(\bar{\mathbf{t}}_{\kappa}))\mathcal{J}_{1,\kappa}^{\alpha,\varphi}\\ +\Big\{\rho_5\mathcal{G}_5(\bar{\mathbf{t}}_{\kappa+1},\mathbf{Q}_{\kappa+1})(\mathbf{B}_5(\bar{\mathbf{t}}_{\kappa+1})-\mathbf{B}_5(\bar{\mathbf{t}}_{\kappa}))\\ -\rho_5\mathcal{G}_5(\bar{\mathbf{t}}_{\kappa},\mathbf{Q}_{\kappa})(\mathbf{B}_5(\bar{\mathbf{t}}_{\kappa})-\mathbf{B}_5(\bar{\mathbf{t}}_{\kappa-1}))\Big\}\mathcal{J}_{2,\kappa}^{\alpha,\varphi}\\ +\Big\{\frac{\rho_5\mathcal{G}_5\left(\bar{\mathbf{t}}_{\kappa+1},\mathbf{Q}_{\kappa+1}\right)\left(\mathbf{B}_5(\bar{\mathbf{t}}_{\kappa+1})-\mathbf{B}_5(\bar{\mathbf{t}}_{\kappa})\right)-2\rho_5\mathcal{G}_5\left(\bar{\mathbf{t}}_{\kappa},\mathbf{Q}_{\kappa}\right)\left(\mathbf{B}_5(\bar{\mathbf{t}}_{\kappa})-\mathbf{B}_5(\bar{\mathbf{t}}_{\kappa-1})\right)}{\hbar}\\ -\frac{\rho_5\mathcal{G}_5\left(\bar{\mathbf{t}}_{\kappa-1},\mathbf{Q}_{\kappa-1}\right)\left(\mathbf{B}_5(\bar{\mathbf{t}}_{\kappa-1})-\mathbf{B}_5(\bar{\mathbf{t}}_{\kappa-2})\right)}{\hbar}\Big\}\mathcal{J}_{3,\kappa}^{\alpha,\varphi}\end{array}\right]\end{aligned}$$

$$+\frac{\alpha\varphi}{\mathbf{ABC}(\alpha)\Gamma(\alpha)}\left[\begin{array}{l}\mathbf{Q}^*(\bar{\mathbf{t}}_{\mathfrak{n}+1},\mathbf{F}_{\mathfrak{n}+1}^p,\mathbf{Q}_{\mathfrak{n}+1}^p)\mathcal{J}_{1,\mathfrak{n}}^{\alpha,\varphi}\\ +\mathbf{Q}^*(\bar{\mathbf{t}}_{\mathfrak{n}+1},\mathbf{F}_{\mathfrak{n}+1}^p,\mathbf{Q}_{\mathfrak{n}+1}^p)\mathcal{J}_{2,\mathfrak{n}}^{\alpha,\varphi}\\ -\mathbf{Q}^*(\bar{\mathbf{t}}_{\mathfrak{n}},\mathbf{F}_{\mathfrak{n}},\mathbf{Q}_{\mathfrak{n}})\mathcal{J}_{2,\mathfrak{n}}^{\alpha,\varphi}\\ +\Big\{\frac{\mathbf{Q}^*\left(\bar{\mathbf{t}}_{\mathfrak{n}+1},\mathbf{F}_{\mathfrak{n}+1}^p,\mathbf{Q}_{\mathfrak{n}+1}^p\right)-2\mathbf{Q}^*\left(\bar{\mathbf{t}}_{\mathfrak{n}},\mathbf{F}_{\mathfrak{n}},\mathbf{Q}_{\mathfrak{n}}\right)}{2\hbar}\Big\}\mathcal{J}_{3,\mathfrak{n}}^{\alpha,\varphi}\\ +\frac{\mathbf{Q}^*\left(\bar{\mathbf{t}}_{\mathfrak{n}-1},\mathbf{F}_{\mathfrak{n}-1},\mathbf{Q}_{\mathfrak{n}-1}\right)}{2\hbar^2}\mathcal{J}_{3,\mathfrak{n}}^{\alpha,\varphi}\\ +\rho_5\mathcal{G}_5(\bar{\mathbf{t}}_{\mathfrak{n}+1},\mathbf{Q}_{\mathfrak{n}+1}^{p_1})(\mathbf{B}_5(\bar{\mathbf{t}}_{\mathfrak{n}+1})-\mathbf{B}_5(\bar{\mathbf{t}}_{\mathfrak{n}}))\mathcal{J}_{1,\mathfrak{n}}^{\alpha,\varphi}\\ +\rho_5\mathcal{G}_5(\bar{\mathbf{t}}_{\mathfrak{n}+1},\mathbf{Q}_{\mathfrak{n}+1}^{p_1})(\mathbf{B}_5(\bar{\mathbf{t}}_{\mathfrak{n}+1})-\mathbf{B}_5(\bar{\mathbf{t}}_{\mathfrak{n}}))\mathcal{J}_{2,\mathfrak{n}}^{\alpha,\varphi}\\ -\rho_5\mathcal{G}_5(\bar{\mathbf{t}}_{\mathfrak{n}},\mathbf{Q}_{\mathfrak{n}}^{p_1})(\mathbf{B}_5(\bar{\mathbf{t}}_{\mathfrak{n}})-\mathbf{B}_5(\bar{\mathbf{t}}_{\mathfrak{n}-1}))\mathcal{J}_{2,\mathfrak{n}}^{\alpha,\varphi}\\ +\frac{\rho_5\mathcal{G}_5\left(\bar{\mathbf{t}}_{\mathfrak{n}+1},\mathbf{Q}_{\mathfrak{n}+1}^{p_1}\right)\left(\mathbf{B}_5(\bar{\mathbf{t}}_{\mathfrak{n}+1})-\mathbf{B}_5(\bar{\mathbf{t}}_{\mathfrak{n}})\right)}{2\hbar}\mathcal{J}_{3,\mathfrak{n}}^{\alpha,\varphi}\\ -2\frac{\rho_5\mathcal{G}_5\left(\bar{\mathbf{t}}_{\mathfrak{n}},\mathbf{Q}_{\mathfrak{n}}^{p_1}\right)\left(\mathbf{B}_5(\bar{\mathbf{t}}_{\mathfrak{n}})-\mathbf{B}_5(\bar{\mathbf{t}}_{\mathfrak{n}-1})\right)}{2\hbar}\mathcal{J}_{3,\mathfrak{n}}^{\alpha,\varphi}\\ +\frac{\rho_5\mathcal{G}_5\left(\bar{\mathbf{t}}_{\mathfrak{n}-1},\mathbf{Q}_{\mathfrak{n}-1}^{p_1}\right)\left(\mathbf{B}_5(\bar{\mathbf{t}}_{\mathfrak{n}-2})-\mathbf{B}_5(\bar{\mathbf{t}}_{\mathfrak{n}-2})\right)}{2\hbar}\mathcal{J}_{3,\mathfrak{n}}^{\alpha,\varphi}\end{array}\right],$$

where

$$
\begin{aligned}
\mathbf{U}_{\mathfrak{n}+1}^{p_1} &= \mathbf{U}_0 + \frac{1-\alpha}{\mathbf{ABC}(\alpha)}\wp\bar{\mathbf{t}}_{\mathfrak{n}+1}^{\wp-1}\left[\begin{cases}\mathbf{U}^*(\bar{\mathbf{t}}_{\mathfrak{n}},\mathbf{U}_{\mathfrak{n}},\mathbf{A}_{\mathfrak{n}},\mathbf{F}_{\mathfrak{n}})\\ +\wp\rho_1\mathcal{G}_1(\bar{\mathbf{t}}_{\mathfrak{n}},\mathbf{U}_{\mathfrak{n}})(\mathbf{B}_1(\bar{\mathbf{t}}_{\mathfrak{n}})-\mathbf{B}_1(\bar{\mathbf{t}}_{\mathfrak{n}-1}))\end{cases}\right]\\
&\quad+\frac{\alpha\wp}{\mathbf{ABC}(\alpha)\Gamma(\alpha)}\sum_{\kappa=0}^{\mathfrak{n}}\left[\begin{cases}\mathbf{U}^*(\bar{\mathbf{t}}_{\kappa},\mathbf{U}_{\kappa},\mathbf{A}_{\kappa},\mathbf{F}_{\kappa})\mathcal{J}_{1,\kappa}^{\alpha,\wp}\\ +\rho_1\mathcal{G}_1(\bar{\mathbf{t}}_{\kappa},\mathbf{U}_{\kappa})(\mathbf{B}_1(\bar{\mathbf{t}}_{\kappa})-\mathbf{B}_1(\bar{\mathbf{t}}_{\kappa-1}))\mathcal{J}_{1,\kappa}^{\alpha,\wp}\end{cases}\right],\\
\mathbf{S}_{\mathfrak{n}+1}^{p_1} &= \mathbf{S}_0 + \frac{1-\alpha}{\mathbf{ABC}(\alpha)}\wp\bar{\mathbf{t}}_{\mathfrak{n}+1}^{\wp-1}\left[\begin{cases}\mathbf{S}^*(\bar{\mathbf{t}}_{\mathfrak{n}},\mathbf{U}_{\mathfrak{n}},\mathbf{S}_{\mathfrak{n}},\mathbf{A}_{\mathfrak{n}},\mathbf{F}_{\mathfrak{n}})\\ +\wp\rho_2\mathcal{G}_2(\bar{\mathbf{t}}_{\mathfrak{n}},\mathbf{S}_{\mathfrak{n}})(\mathbf{B}_2(\bar{\mathbf{t}}_{\mathfrak{n}})-\mathbf{B}_2(\bar{\mathbf{t}}_{\mathfrak{n}-1}))\end{cases}\right]\\
&\quad+\frac{\alpha\wp}{\mathbf{ABC}(\alpha)\Gamma(\alpha)}\sum_{\kappa=0}^{\mathfrak{n}}\left[\begin{cases}\mathbf{S}^*(\bar{\mathbf{t}}_{\kappa},\mathbf{U}_{\kappa},\mathbf{S}_{\kappa},\mathbf{A}_{\kappa},\mathbf{F}_{\kappa})\mathcal{J}_{1,\kappa}^{\alpha,\wp}\\ +\rho_2\mathcal{G}_2(\bar{\mathbf{t}}_{\kappa},\mathbf{S}_{\kappa})(\mathbf{B}_2(\bar{\mathbf{t}}_{\kappa})-\mathbf{B}_2(\bar{\mathbf{t}}_{\kappa-1}))\mathcal{J}_{1,\kappa}^{\alpha,\wp}\end{cases}\right],\\
\mathbf{A}_{\mathfrak{n}+1}^{p_1} &= \mathbf{A}_0 + \frac{1-\alpha}{\mathbf{ABC}(\alpha)}\wp\bar{\mathbf{t}}_{\mathfrak{n}+1}^{\wp-1}\left[\begin{cases}\mathbf{A}^*(\bar{\mathbf{t}}_{\mathfrak{n}},\mathbf{U}_{\mathfrak{n}},\mathbf{S}_{\mathfrak{n}},\mathbf{A}_{\mathfrak{n}},\mathbf{F}_{\mathfrak{n}})\\ +\wp\rho_3\mathcal{G}_3(\bar{\mathbf{t}}_{\mathfrak{n}},\mathbf{A}_{\mathfrak{n}})(\mathbf{B}_3(\bar{\mathbf{t}}_{\mathfrak{n}})-\mathbf{B}_3(\bar{\mathbf{t}}_{\mathfrak{n}-1}))\end{cases}\right]\\
&\quad+\frac{\alpha\wp}{\mathbf{ABC}(\alpha)\Gamma(\alpha)}\sum_{\kappa=0}^{\mathfrak{n}}\left[\begin{cases}\mathbf{A}^*(\bar{\mathbf{t}}_{\kappa},\mathbf{U}_{\kappa},\mathbf{S}_{\kappa},\mathbf{A}_{\kappa},\mathbf{F}_{\kappa})\mathcal{J}_{1,\kappa}^{\alpha,\wp}\\ +\rho_3\mathcal{G}_3(\bar{\mathbf{t}}_{\kappa},\mathbf{A}_{\kappa})(\mathbf{B}_3(\bar{\mathbf{t}}_{\kappa})-\mathbf{B}_3(\bar{\mathbf{t}}_{\kappa-1}))\mathcal{J}_{1,\kappa}^{\alpha,\wp}\end{cases}\right],\\
\mathbf{F}_{\mathfrak{n}+1}^{p_1} &= \mathbf{F}_0 + \frac{1-\alpha}{\mathbf{ABC}(\alpha)}\wp\bar{\mathbf{t}}_{\mathfrak{n}+1}^{\wp-1}\left[\begin{cases}\mathbf{F}^*(\bar{\mathbf{t}}_{\mathfrak{n}},\mathbf{A}_{\mathfrak{n}},\mathbf{F}_{\mathfrak{n}},\mathbf{Q}_{\mathfrak{n}})\\ +\wp\rho_4\mathcal{G}_4(\bar{\mathbf{t}}_{\mathfrak{n}},\mathbf{F}_{\mathfrak{n}})(\mathbf{B}_4(\bar{\mathbf{t}}_{\mathfrak{n}})-\mathbf{B}_4(\bar{\mathbf{t}}_{\mathfrak{n}-1}))\end{cases}\right]\\
&\quad+\frac{\alpha\wp}{\mathbf{ABC}(\alpha)\Gamma(\alpha)}\sum_{\kappa=0}^{\mathfrak{n}}\left[\begin{cases}\mathbf{F}^*(\bar{\mathbf{t}}_{\kappa},\mathbf{A}_{\kappa},\mathbf{F}_{\kappa},\mathbf{Q}_{\kappa})\mathcal{J}_{1,\kappa}^{\alpha,\wp}\\ +\rho_4\mathcal{G}_4(\bar{\mathbf{t}}_{\kappa},\mathbf{F}_{\kappa})(\mathbf{B}_4(\bar{\mathbf{t}}_{\kappa})-\mathbf{B}_4(\bar{\mathbf{t}}_{\kappa-1}))\mathcal{J}_{1,\kappa}^{\alpha,\wp}\end{cases}\right],\\
\mathbf{Q}_{\mathfrak{n}+1}^{p_1} &= \mathbf{Q}_0 + \frac{1-\alpha}{\mathbf{ABC}(\alpha)}\wp\bar{\mathbf{t}}_{\mathfrak{n}+1}^{\wp-1}\left[\begin{cases}\mathbf{Q}^*(\bar{\mathbf{t}}_{\mathfrak{n}},\mathbf{F}_{\mathfrak{n}},\mathbf{Q}_{\mathfrak{n}})\\ +\wp\rho_5\mathcal{G}_5(\bar{\mathbf{t}}_{\mathfrak{n}},\mathbf{Q}_{\mathfrak{n}})(\mathbf{B}_5(\bar{\mathbf{t}}_{\mathfrak{n}})-\mathbf{B}_5(\bar{\mathbf{t}}_{\mathfrak{n}-1}))\end{cases}\right]\\
&\quad+\frac{\alpha\wp}{\mathbf{ABC}(\alpha)\Gamma(\alpha)}\sum_{\kappa=0}^{\mathfrak{n}}\left[\begin{cases}\mathbf{Q}^*(\bar{\mathbf{t}}_{\kappa},\mathbf{F}_{\kappa},\mathbf{Q}_{\kappa})\mathcal{J}_{1,\kappa}^{\alpha,\wp}\\ +\rho_5\mathcal{G}_5(\bar{\mathbf{t}}_{\kappa},\mathbf{Q}_{\kappa})(\mathbf{B}_5(\bar{\mathbf{t}}_{\kappa})-\mathbf{B}_5(\bar{\mathbf{t}}_{\kappa-1}))\mathcal{J}_{1,\kappa}^{\alpha,\wp}\end{cases}\right].
\end{aligned}
$$

Also,

$$
\begin{aligned}
\mathcal{J}_{1,\kappa}^{\alpha,\wp} &= \frac{((\mathfrak{n}+1)\hbar)^{\alpha-1}}{\wp}\left[\begin{cases}((\kappa+1)\hbar)^{\wp}\,{}_2\mathcal{F}_1\Big([\wp,1-\alpha],[1+\wp],\frac{\kappa+1}{\mathfrak{n}+1}\Big)\\ -(\kappa\hbar)^{\wp}\,{}_2\mathcal{F}_1\Big([\wp,1-\alpha],[1+\wp],\frac{\kappa}{\mathfrak{n}}\Big)\end{cases}\right],\\
\mathcal{J}_{2,\kappa}^{\alpha,\wp} &= \frac{((\mathfrak{n}+1)\hbar)^{\alpha-1}}{\wp(\wp+1)}\left[\begin{cases}\wp((\kappa+1)\hbar)^{\wp+1}\,{}_2\mathcal{F}_1\Big([1+\wp,1-\alpha],[2+\wp],\frac{\kappa+1}{\mathfrak{n}+1}\Big)\\ -(1+\wp)((\kappa+1)\hbar)^{\wp+1}\,{}_2\mathcal{F}_1\Big([\wp,1-\alpha],[1+\wp],\frac{\kappa+1}{\mathfrak{n}}\Big)\\ -\wp((\kappa)\hbar)^{\wp+1}\,{}_2\mathcal{F}_1\Big([1+\wp,1-\alpha],[2+\wp],\frac{\kappa}{\mathfrak{n}+1}\Big)\\ +\hbar((\kappa)\hbar)^{\wp}(1+\wp)(1+\kappa)\,{}_2\mathcal{F}_1\Big([\wp,1-\alpha],[1+\wp],\frac{\kappa}{\mathfrak{n}}\Big)\end{cases}\right],
\end{aligned}
$$

$$\mathcal{J}_{3,\kappa}^{\alpha,\wp} = \frac{((\kappa+1)\hbar)^{\alpha-1}}{\wp(\wp+1)(\wp+2)} \left[\begin{cases} \wp(\wp+1)((\kappa+1)\hbar)^{\wp+2}\, {}_2\mathcal{F}_1\Big([2+\wp, 1-\alpha], [3+\wp], \frac{\kappa+1}{\mathfrak{n}+1}\Big) \\ -2\wp(\wp+2)\Big(\kappa+\frac{1}{2}\Big)\hbar((\kappa+1)\hbar)^{\wp+1}\, {}_2\mathcal{F}_1\Big([1+\wp, 1-\alpha], [2+\wp], \frac{\kappa+1}{\mathfrak{n}+1}\Big) \\ +\kappa\hbar(\wp+1)(\wp+2)((\kappa+1)\hbar)^{\wp+1}\, {}_2\mathcal{F}_1\Big([\wp, 1-\alpha], [1+\wp], \frac{\kappa+1}{\mathfrak{n}}\Big) \\ +2\wp(\wp+2)\Big(\kappa+\frac{1}{2}\Big)\hbar((\hbar\kappa))^{\wp+1}\, {}_2\mathcal{F}_1\Big([1+\wp, 1-\alpha], [2+\wp], \frac{\kappa}{\mathfrak{n}+1}\Big) \\ -\wp(\wp+1)(\kappa\hbar)^{\wp+2}\, {}_2\mathcal{F}_1\Big([2+\wp, 1-\alpha], [3+\wp], \frac{\kappa}{\mathfrak{n}}\Big) \\ -\hbar(\wp+1)(\wp+2)(\kappa+1)(\kappa\hbar)^{\wp+1}\, {}_2\mathcal{F}_1\Big([\wp, 1-\alpha], [1+\wp], \frac{\kappa}{\mathfrak{n}+1}\Big) \end{cases} \right].$$

6. Results and discussion

To exemplify the theoretical outcomes of the suggested framework, numerical computations were performed in this part. We accomplish this using the stochastic complete numerical technique proposed by Atangana and Araz [52]. Moreover, we compute the fractal-fractional model (3.2) for Atangana-Baleanu-Caputo sense when both fractional-order α and fractal-dimension $\wp$ are distinct.

Figures 3–5 illustrate the effects of uninfected $\mathbf{U}(\bar{\mathbf{t}})$, latently infected $\mathbf{S}(\bar{\mathbf{t}})$, actively infected $\mathbf{A}(\bar{\mathbf{t}})$, free virus $\mathbf{F}(\bar{\mathbf{t}})$, and antibodies $\mathbf{Q}(\bar{\mathbf{t}})$ at various fractional-orders and fixed fractal-dimensions. We assign the following parameter values: $\Lambda = 10$, $\varsigma = 0.1$, $\lambda_1 = 2$, $\lambda_2 = 2$, $\phi = 0.5$, $\nu_1 = 0.5$, $\sigma = 5$, $\delta = 10$, $\varphi = 2$, $\nu_2 = 10$, $\xi = 3$, $\chi = 2$, $\zeta = 4$. To demonstrate the system's dynamical behaviour, we input various white noise levels (5.1). We first take into account the white noise components $\rho_1 = 0.9$, $\rho_2 = 0.9$, $\rho_3 = 0.7$, $\rho_4 = 0.9$ and $\rho_5 = 0.8$, where the distinctive stationary distribution sensitivity criterion $\mathbb{R}_0^s > 1$ is attained. As the virus spreads through the community, the class diminishes over time and eventually affects all other categories in the structure. This classification corresponds rapidly at low orders and slowly at higher orders, which displays a consistent tendency.

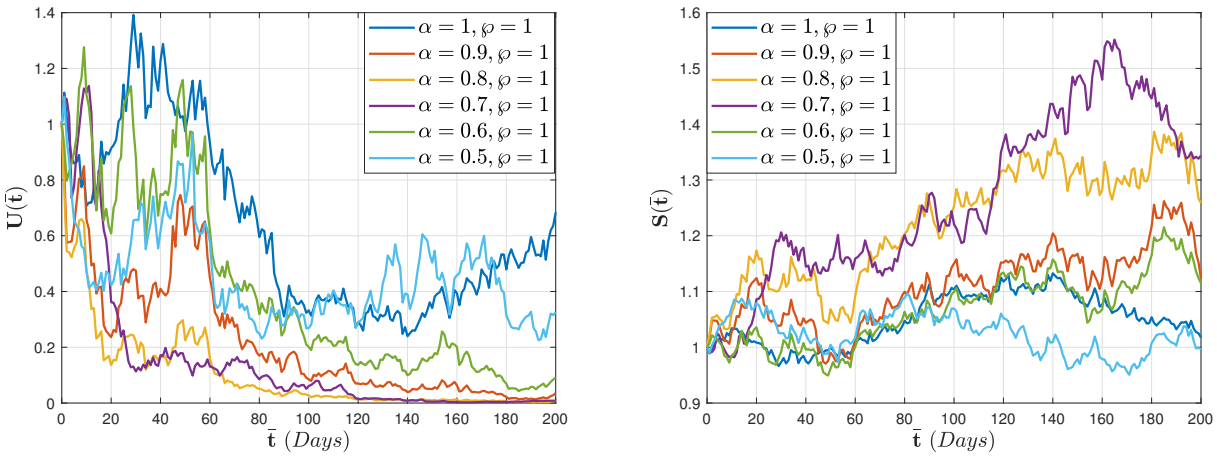

(a) **(b)**

Figure 3. Graphical display of uninfected cells $\mathbf{U}(\bar{\mathbf{t}})$ and latently infected cells $\mathbf{S}(\bar{\mathbf{t}})$ of the model (5.1) considering the fractal-fractional derivative with generalized Mittag-Leffler kernel and varying fractional-order with fixed fractal-dimension.

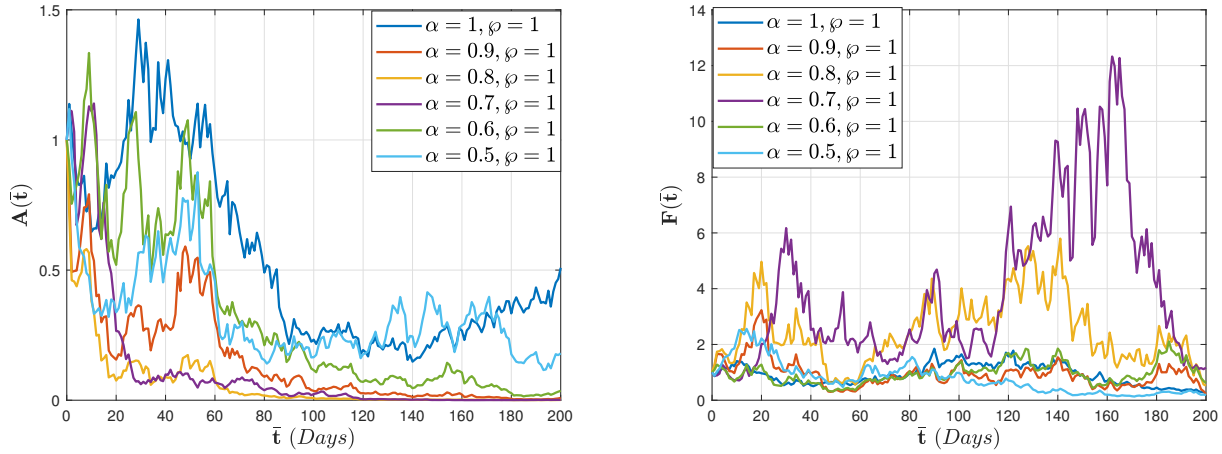

(a) **(b)**

Figure 4. Graphical display of actively infected cells $\mathbf{A}(\bar{\mathbf{t}})$ and free virus $\mathbf{F}(\bar{\mathbf{t}})$ of the model (5.1) considering the fractal-fractional derivative with generalized Mittag-Leffler kernel and varying fractional-order with fixed fractal-dimension.

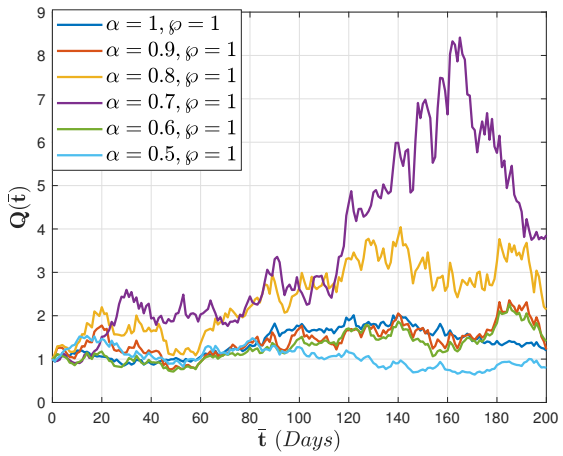

(a)

Figure 5. Graphical display of antibodies $\mathbf{Q}(\bar{\mathbf{t}})$ of the model (5.1) considering the fractal-fractional derivative with generalized Mittag-Leffler kernel and varying fractional-order with fixed fractal-dimension.

Figures 6–8 display the temporal patterns of $(\mathbf{U}(\bar{\mathbf{t}}), \mathbf{S}(\bar{\mathbf{t}}), \mathbf{A}(\bar{\mathbf{t}}), \mathbf{F}(\bar{\mathbf{t}}), \mathbf{Q}(\bar{\mathbf{t}}))$ of the stochastic system (5.1) involving white noise $\rho_1 = 0.9$, $\rho_2 = 0.9$, $\rho_3 = 0.7$, $\rho_4 = 0.9$ and $\rho_5 = 0.8$, respectively. The solution varies at white noises, having a corresponding stochastic mean. The affected cells $\mathbf{S}(\bar{\mathbf{t}})$ exhibit a rapid decline in behaviour over time, similar to the behaviour of uninfected cells $\mathbf{U}(\bar{\mathbf{t}})$ at various fractal-fractional orders.

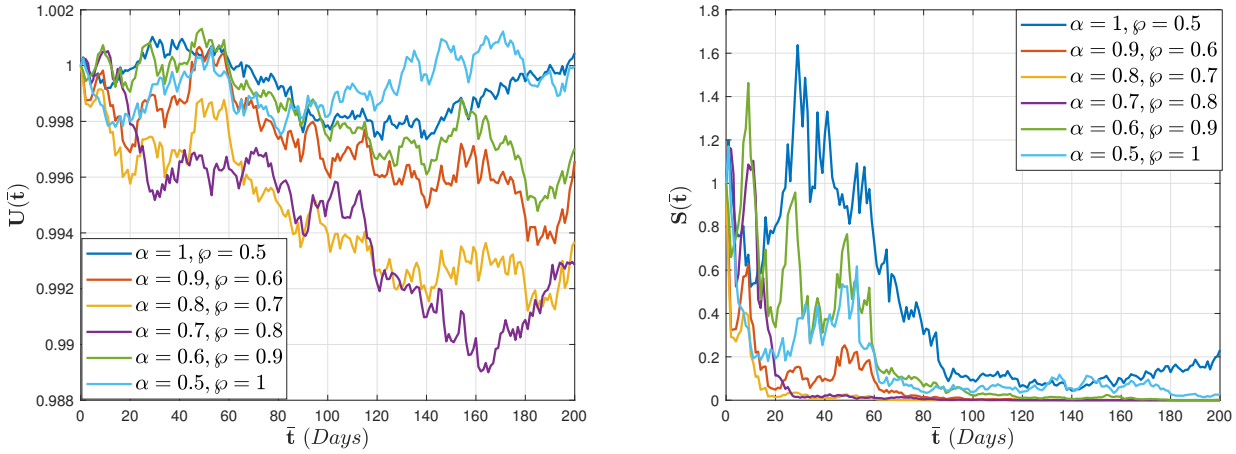

(a) **(b)**

Figure 6. Graphical display of uninfected cells $\mathbf{U}(\bar{\mathbf{t}})$ and latently infected cells $\mathbf{S}(\bar{\mathbf{t}})$ of the model (5.1) considering the fractal-fractional derivative with generalized Mittag-Leffler kernel and varying both fractional-order with fractal-dimension.

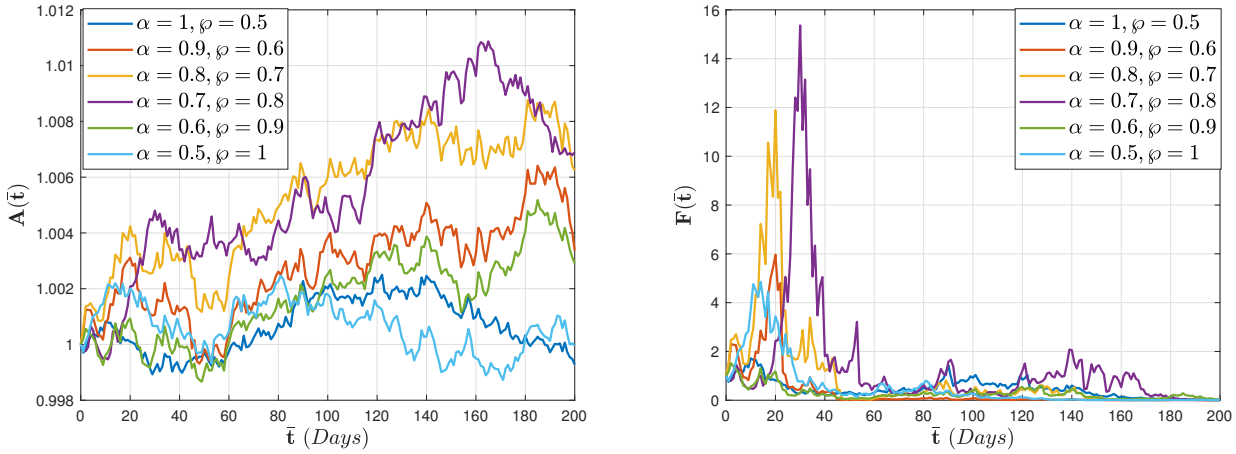

(a) **(b)**

Figure 7. Graphical display of actively infected cells $\mathbf{A}(\bar{\mathbf{t}})$ and free virus $\mathbf{F}(\bar{\mathbf{t}})$ of the model (5.1) considering the fractal-fractional derivative with generalized Mittag-Leffler kernel and varying both fractional-order with fractal-dimension.

Figures 9–11 show the impacts of uninfected $\mathbf{U}(\bar{\mathbf{t}})$, latently infected $\mathbf{S}(\bar{\mathbf{t}})$, actively infected $\mathbf{A}(\bar{\mathbf{t}})$, free virus $\mathbf{F}(\bar{\mathbf{t}})$, and antibodies $\mathbf{Q}(\bar{\mathbf{t}})$ at various fractal-dimension and fixed fractional-orders. The corresponding attributed values: $\Lambda = 10$, $\varsigma = 0.1$, $\lambda_1 = 2$, $\lambda_2 = 2$, $\phi = 0.5$, $\nu_1 = 0.5$, $\sigma = 5$, $\delta = 10$, $\varphi = 2$, $\nu_2 = 10$, $\xi = 3$, $\chi = 2$, $\zeta = 4$. Then, by increasing the white noise intensities to $\rho_1 = 3.9$, $\rho_2 = 3.7$, $\rho_3 = 3.9$, $\rho_4 = 3.9$ and $\rho_5 = 3.8$, we are able to satisfy the elimination criterion $\tilde{\mathbb{R}}_0^s < 1$ in Theorem 4.3 and validate the findings. Figures 9–11 demonstrate that as the white noise intensity escalates, contaminated lymphocytes $\mathbf{S}(\bar{\mathbf{t}})$, productively infested cells $\mathbf{A}(\bar{\mathbf{t}})$, and uncontrolled

pathogen $\mathbf{A}(\bar{\mathbf{t}})$ can all perish and settle at a variety of fractal dimensions and fixed fractional-order. This shows that white noise concentration can effectively eradicate all insidiously, proactively, and freely virally infested cells, dramatically reduce the quantity of virally affected cells, and prevent the proliferation of contaminated nuclei.

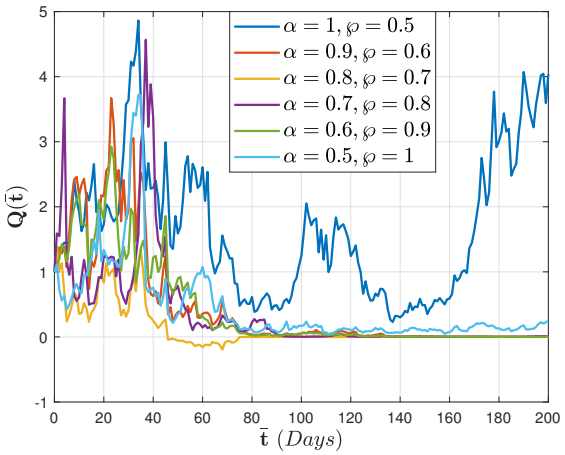

(a)

Figure 8. Graphical display of antibodies $\mathbf{Q}(\bar{\mathbf{t}})$ of the model (5.1) considering the fractal-fractional derivative with generalized Mittag-Leffler kernel and varying both fractional-order with fractal-dimension.

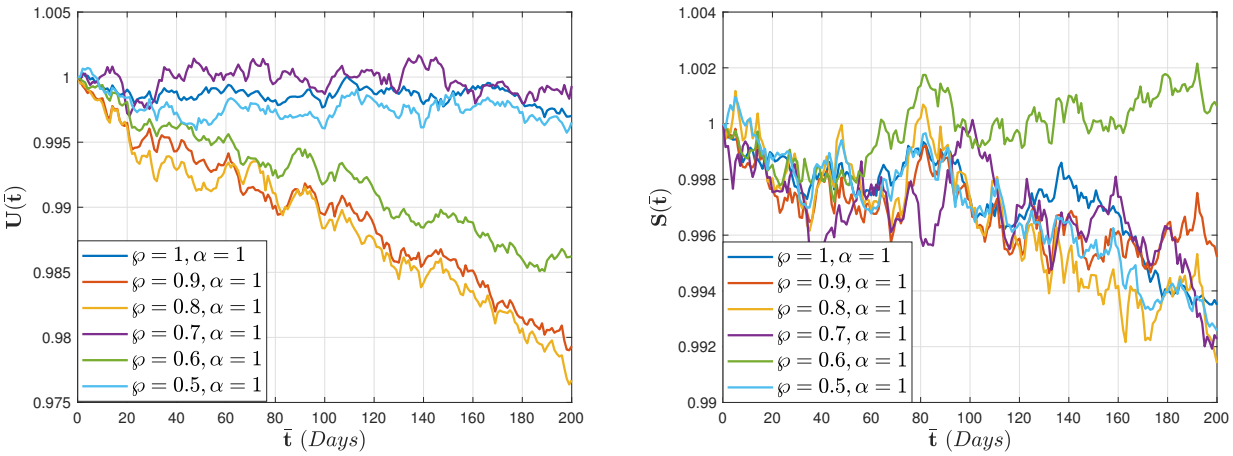

(a) **(b)**

Figure 9. Graphical display of uninfected cells $\mathbf{U}(\bar{\mathbf{t}})$ and latently infected cells $\mathbf{S}(\bar{\mathbf{t}})$ of the model (5.1) considering the fractal-fractional derivative with generalized Mittag-Leffler kernel and varying fractal-dimension with fixed fractional-order.

Figures 12–14 predict the behaviour of uninfected $\mathbf{U}(\bar{\mathbf{t}})$, latently infected $\mathbf{S}(\bar{\mathbf{t}})$, actively infected $\mathbf{A}(\bar{\mathbf{t}})$, free virus $\mathbf{F}(\bar{\mathbf{t}})$, and antibodies $\mathbf{Q}(\bar{\mathbf{t}})$ at various fractal-dimension and fractional-orders. The corresponding attributed values: $\Lambda = 10$, $\varsigma = 0.1$, $\lambda_1 = 2$, $\lambda_2 = 2$, $\phi = 0.5$, $\nu_1 = 0.5$, $\sigma = 5$, $\delta =$

10, $\varphi = 2$, $\nu_2 = 10$, $\xi = 3$, $\chi = 2$, $\zeta = 4$. Then, by increasing the white noise intensities to $\rho_1 = 3.9$, $\rho_2 = 3.7$, $\rho_3 = 3.9$, $\rho_4 = 3.9$ and $\rho_5 = 3.8$, and $\tilde{\mathbb{R}}_0^s < 1$. This shows that the stochastic noise is demonstrated to be suppressed by the massive boom. The infectious populace is disappearing more significantly when both fractional-order and fractal-dimension are changed simultaneously in an infectious system in comparison to fractional systems, which leads to fascinating and biologically more plausible findings.

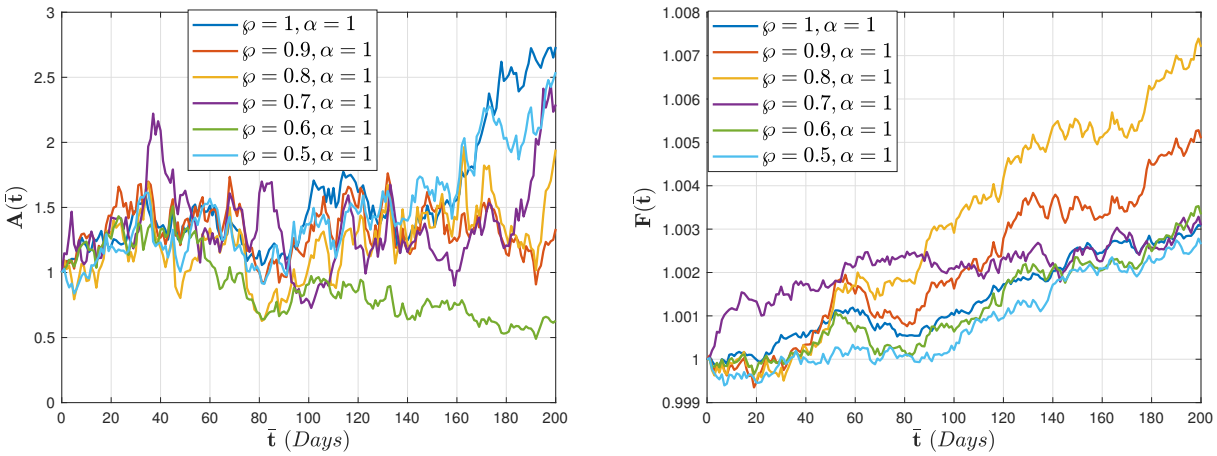

(a) **(b)**

Figure 10. Graphical display of actively infected cells $\mathbf{A}(\bar{t})$ and free virus $\mathbf{F}(\bar{t})$ of the model (5.1) considering the fractal-fractional derivative with generalized Mittag-Leffler kernel and varying fractal-dimension with fixed fractional-order.

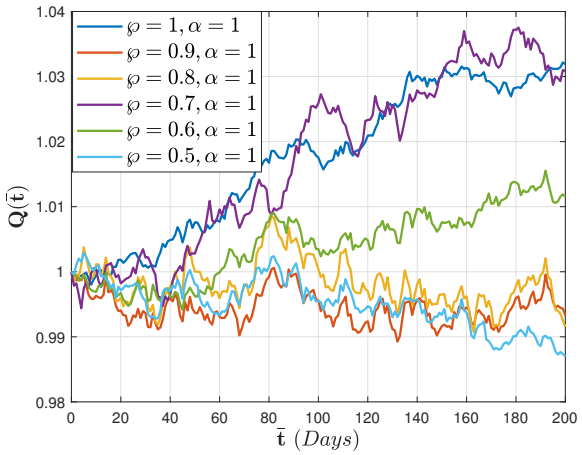

(a)

Figure 11. Graphical display of antibodies $\mathbf{Q}(\bar{t})$ of the model (5.1) considering the fractal-fractional derivative with generalized Mittag-Leffler kernel and varying fractal-dimension with fixed fractional-order.

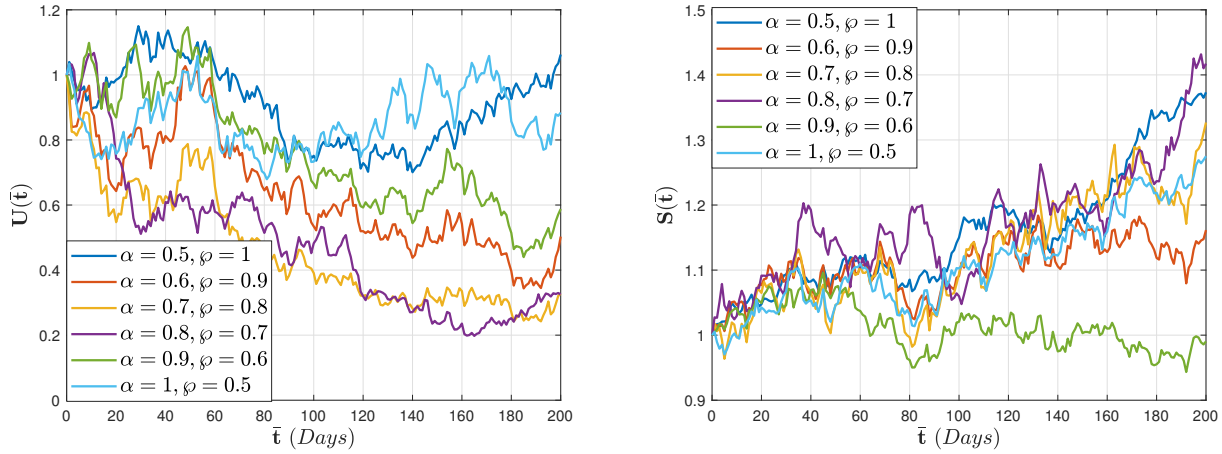

(a) **(b)**

Figure 12. Graphical display of uninfected cells $\mathbf{U}(\bar{t})$ and latently infected cells $\mathbf{S}(\bar{t})$ of the model (5.1) considering the fractal-fractional derivative with generalized Mittag-Leffler kernel and both varying fractal-dimension with fractional-order.

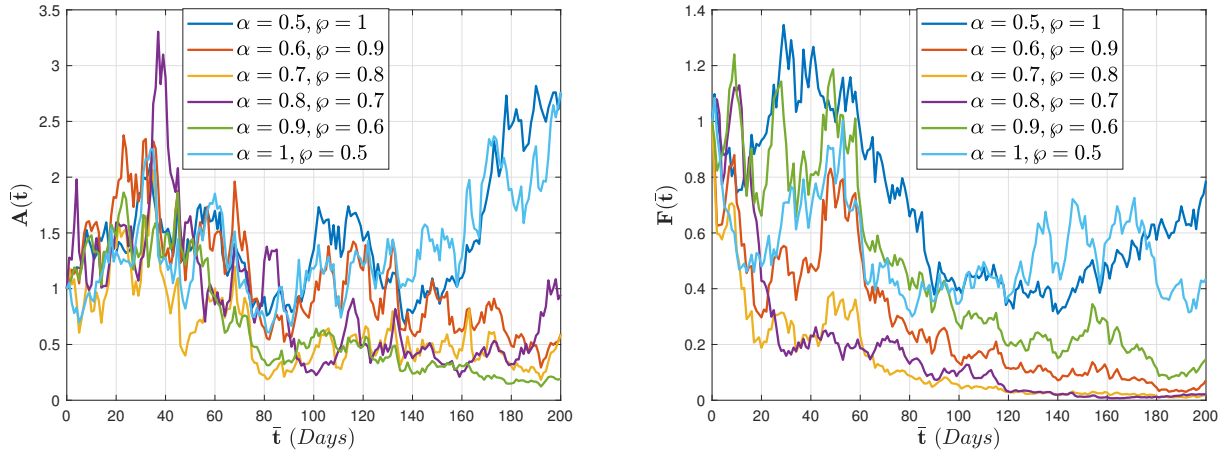

(a) **(b)**

Figure 13. Graphical display of actively infected cells $\mathbf{A}(\bar{t})$ and free virus $\mathbf{F}(\bar{t})$ of the model (5.1) considering the fractal-fractional derivative with generalized Mittag-Leffler kernel and both varying fractal-dimension with fractional-order.

Figures 15–17 demonstrate the effect of uninfected $\mathbf{U}(\bar{t})$, latently infected $\mathbf{S}(\bar{t})$, actively infected $\mathbf{A}(\bar{t})$, free virus $\mathbf{F}(\bar{t})$, and antibodies $\mathbf{Q}(\bar{t})$ at fixed fractal-dimension and fractional-orders with and without control, respectively. Considering an inadequate CTL reaction, we examine how virus replication affects the patterns of HCV and immunological reactions from acute infection through the chronic stage. This is accomplished using a mix of analytical and numerical techniques. Since the target cell restriction prevents the penetration of new viral variations in the case of severe liver damage, virus development is predicted to come to an end.

As a result of these pictorial outcomes, we draw the conclusion that by using this novel fractal-fractional operator concept, it is possible to detect more precise outcomes and to offer a wider insight of problems that arise in engineering and science as well as in the reality.

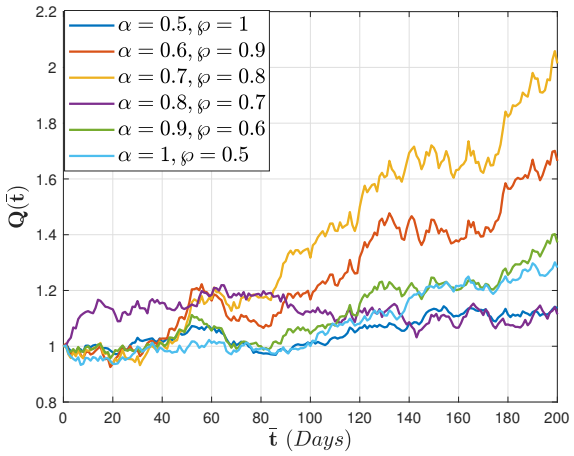

(a)

Figure 14. Graphical display of antibodies $\mathbf{Q}(\bar{\mathbf{t}})$ of the model (5.1) considering the fractal-fractional derivative with generalized Mittag-Leffler kernel and both varying fractal-dimension with fractional-order.

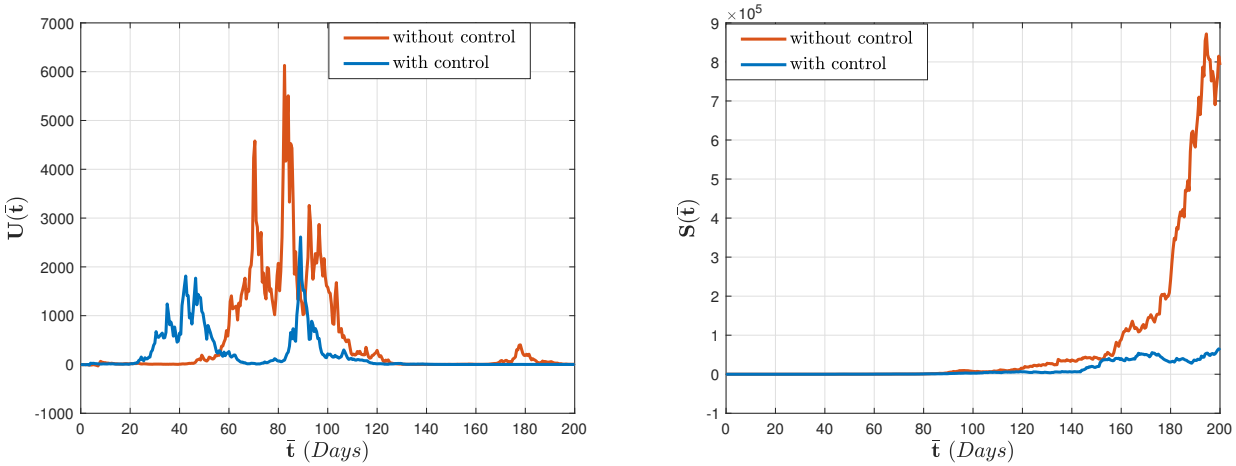

(a) **(b)**

Figure 15. Graphical display of uninfected cells $\mathbf{U}(\bar{\mathbf{t}})$ and latently infected cells $\mathbf{S}(\bar{\mathbf{t}})$ of the model (5.1) with and without control when $\alpha = 0.98$ considering the fractal-fractional derivative with generalized Mittag-Leffler kernel.

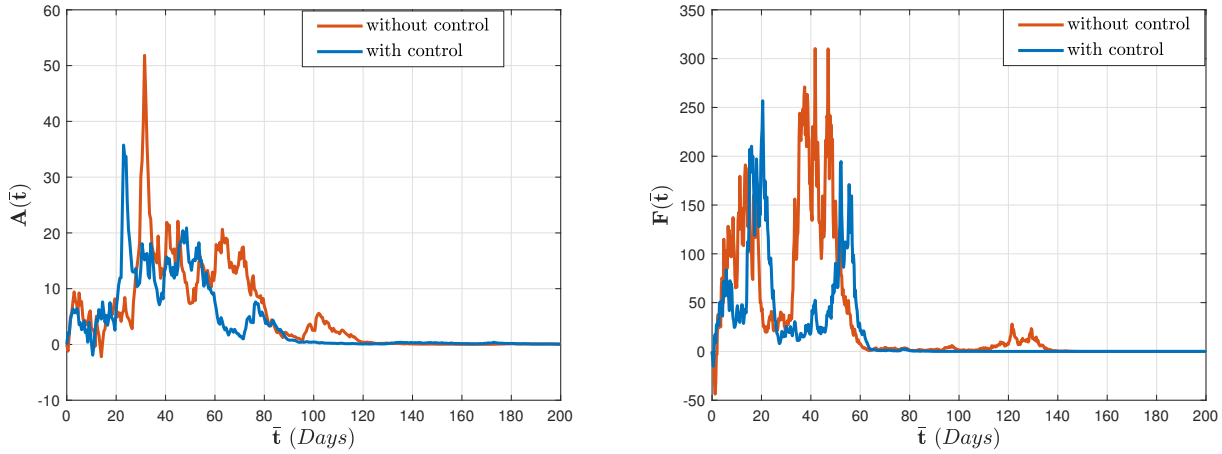

(a) **(b)**

Figure 16. Graphical display of actively infected cells $\mathbf{A}(\bar{\mathbf{t}})$ and free virus $\mathbf{F}(\bar{\mathbf{t}})$ of the model (5.1) with and without control when $\alpha = 0.98$ considering the fractal-fractional derivative with generalized Mittag-Leffler kernel.

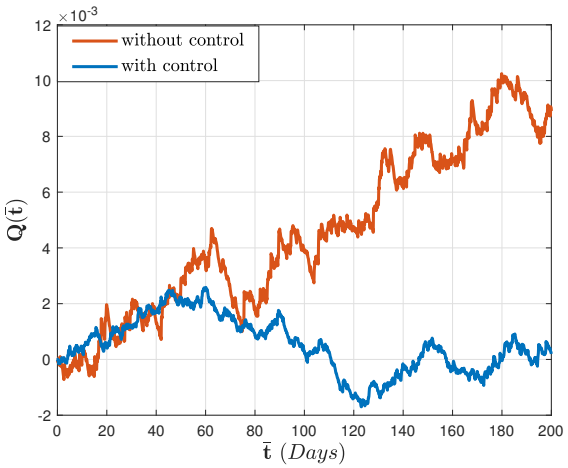

(a)

Figure 17. Graphical display of antibodies $\mathbf{Q}(\bar{\mathbf{t}})$ of the model (5.1) with and without control when $\alpha = 0.98$ considering the fractal-fractional derivative with generalized Mittag-Leffler kernel.

7. Conclusions

In this article, we examined the variations in cellular complexities of a novel randomized fractal-fractional virus transmission system considering latently diseased tissues and a Holling type II functionality reaction. We discovered the existence of non-negative solutions to the examined system by accounting for environmental noise and the fractal effects of vaccination. In view of Itô's technique and Lyapunov candidate, we established the necessary assumptions of the stochastically permanence of

the virus transmission scenario and the elimination of chronically diseased, productively contaminated cells and independent pathogen fragments. Ultimately, in order to create the suggested system, we employed the F-F calculus notion in the ABC context. Additionally, numerical simulations are provided to understand the tendencies of our theoretical model's analysis. We determine that increasing the noise strength will eventually render the virus obsolete. The illustration analysis shows that the fractal-fractional notion outperforms the integer-order and classical derivatives in terms of effectiveness and biological dependability. Upcoming research on viral infections, particularly the novel COVID-19, monkey pox and lumpy virus can confidently implement the revolutionary modelling methodology termed as the fractal-fractional operator.

Conflict of interest

The authors declare there is no conflict of interest.

References

1. S. Cassels, S. J. Clark, M. Morris, Mathematical models for HIV transmission dynamics, *J. Acquired Immune Defic. Syndr.*, **47** (2008), S34–S39. https://doi.org/10.1097/QAI.0b013e3181605da3
2. O. S. Deep, S. Nallamalli, L. N. S. Naik, G. V. SaiTeja, Mathematical model for transmission of Ebola, *Procedia Comput. Sci.*, **48** (2015), 741–745. https://doi.org/10.1016/j.procs.2015.04.210
3. A. Zeb, E. Alzahrani, V. S. Erturk, G. Zaman, Mathematical model for coronavirus disease 2019 (COVID-19) containing isolation class, *Biomed. Res. Int.*, **2020** (2020), 1–7. https://doi.org/10.1155/2020/3452402
4. M. A. Khan, Dengue infection modeling and its optimal control analysis in East Java, Indonesia, *Heliyon*, **7** (2021), e06023. https://doi.org/10.1016/j.heliyon.2021.e06023
5. S. Banerjee, N. Gupta, P. Kodan, A. Mittal, Y. Ray, N. Nischal, et al., Nipah virus disease: A rare and intractable disease, *Intractable Rare Dis. Res.*, **8** (2019), 1–8. https://doi.org/10.5582/irdr.2018.01130
6. S. Zhao, Z. Xu, Y. Lu, A mathematical model of hepatitis B virus transmission and its application for vaccination strategy in China, *Int. J. Epidemiol.*, **29** (2000), 744–752. https://doi.org/10.1093/ije/29.4.744
7. S. Seewaldt, H. E. Thomas, M. Ejrnaes, U. Christen, T. Wolfe, E. Rodrigo, et al., Virus-induced autoimmune diabetes: Most beta-cells die through inflammatory cytokines and not perforin from autoreactive (anti-viral) cytotoxic T-lymphocytes, *Diabetes*, **49** (2000), 1801–1809. https://doi.org/10.2337/diabetes.49.11.1801
8. M. Eichelberger, W. Allan, M. Zijlstra, R. Jaenisch, P. C. Doherty, Clearance of influenza virus respiratory infection in mice lacking class I major histocompatibility complex-restricted CD8+ T cells, *J. Exp. Med.*, **174** (1994), 875–880. https://doi.org/10.1084/jem.174.4.875
9. D. J. Topham, R. A. Tripp, P. C. Doherty, CD8+ T cells clear influenza virus by perforin or Fas-dependent processes, *J. Immunol.*, **159** (1997), 5197–5200.

10. S. Pan, S. P. Chakrabarty, Threshold dynamics of HCV model with cell-to-cell transmission and a non-cytolytic cure in the presence of humoral immunity, *Commun. Nonlinear Sci. Numer. Simul.*, **61** (2018), 180–197. https://doi.org/10.1016/j.cnsns.2018.02.010

11. A. M. Elaiw, N. H. AlShamrani, Global properties of nonlinear humoral immunity viral infection models, *Int. J. Biomath.*, **8** (2015), 1550058. https://doi.org/10.1142/S1793524515500588

12. Y. Luo, L. Zhang, T. Zheng, Z. Teng, Analysis of a diffusive virus infection model with humoral immunity, cell-to-cell transmission and nonlinear incidence, *Physica A*, **535** (2019), 122415. https://doi.org/10.1016/j.physa.2019.122415

13. Y. Wang, M. Lu, D. Jiang, Viral dynamics of a latent HIV infection model with Beddington-DeAngelis incidence function, B-cell immune response and multiple delays, *Math. Biosci. Eng.*, **18** (2021), 274–299. https://doi.org/10.3934/mbe.2021014

14. K. Hattaf, Global stability and Hopf bifurcation of a generalized viral infection model with multi-delays and humoral immunity, *Physica A*, **545** (2020), 123689. https://doi.org/10.1016/j.physa.2019.123689

15. C. Rajivganthi, F. A. Rihan, Global dynamics of a stochastic viral infection model with latently infected cells, *Appl. Sci.*, **11** (2021), 10484. https://doi.org/10.3390/app112110484

16. O. Olaide, A. E. S. Ezugwu, T. Mohamed, L. Abualigah, Ebola optimization search algorithm: A new nature-inspired metaheuristic optimization algorithm, *IEEE Access*, **10** (2022), 1–38. https://doi.org/10.1109/ACCESS.2022.3147821

17. A. E. Ezugwu, J. O. Agushaka, L. Abualigah, S. Mirjalili, A. H. Gandomi, Prairie dog optimization algorithm, *Neural Comput. Appl.*, **2022** (2022), 1–49. https://doi.org/10.1007/s00521-022-07530-9

18. J. O. Agushaka, A. E. Ezugwu, L. Abualigah, Dwarf mongoose optimization algorithm, *Comput. Methods Appl. Mech. Eng.*, **391** (2022), 114570. https://doi.org/10.1016/j.cma.2022.114570

19. L. Abualigah, D. Yousri, M. A. Elaziz, A. A. Ewees, M. A. Al-qaness, A. H. Gandom, Aquila optimizer: A novel meta-heuristic optimization algorithm, Reptile Search Algorithm (RSA), *Comput. Ind. Eng.*, **157** (2021), 107250, https://doi.org/10.1016/j.cie.2021.107250

20. M. E. Omaba, Growth moment, stability and asymptotic behaviours of solution to a class of time-fractal-fractional stochastic differential equation, *Chaos Solitons Fractals*, **147** (2021), 110958. https://doi.org/10.1016/j.chaos.2021.110958

21. M. Gao, D. Jiang, X. Wen, Stationary distribution and extinction for a stochastic two-compartment model of B-cell chronic lymphocytic leukemia, *Int. J. Biomath.*, **14** (2021), 2150065. https://doi.org/10.1142/S1793524521500650

22. Q. Liu, D. Jiang, Dynamical behavior of a stochastic multigroup staged-progression HIV model with saturated incidence rate and higher-order perturbations, *Int. J. Biomath.*, **14** (2021), 2150051. https://doi.org/10.1142/S1793524521500510

23. C. Gokila, M. Sambath, The threshold for a stochastic within-host CHIKV virus model with saturated incidence rate, *Int. J. Biomath.*, **14** (2021), 2150042. https://doi.org/10.1142/S179352452150042X

24. L. Abualigah, A. Diabat, P. Sumari, A. H. Gandomi, Applications, deployments, and integration of internet of drones (IoD), *IEEE Sens. J.*, **99** (2021), 25532–25546. https://doi.org/10.1109/JSEN.2021.3114266

25. T. H. Zhao, O. Castillo, H. Jahanshahi, A. Yusuf, M. O. Alassafi, F. E. Alsaadi, et al., A fuzzy-based strategy to suppress the novel coronavirus (2019-NCOV) massive outbreak, *Appl. Comput. Math.*, **20** (2021), 160–176.

26. K. S. Miller, B. Ross, *An Introduction to the Fractional Calculus and Fractional Differential Equations*, Wiley, 1993.

27. T. H. Zhao, M. I. Khan, Y. M. Chu, Artificial neural networking (ANN) analysis for heat and entropy generation in flow of non-Newtonian fluid between two rotating disks, *Math. Methods Appl. Sci.*, **2021** (2021). https://doi.org/10.1002/mma.7310

28. K. Karthikeyan, P. Karthikeyan, H. M. Baskonus, K. Venkatachalam, Y. M. Chu, Almost sectorial operators on Ψ-Hilfer derivative fractional impulsive integro-differential equations, *Math. Methods Appl. Sci.*, **2021** (2021). https://doi.org/10.1002/mma.7954

29. Y. M. Chu, U. Nazir, M. Sohail, M. M. Selim, J. R. Lee, Enhancement in thermal energy and solute particles using hybrid nanoparticles by engaging activation energy and chemical reaction over a parabolic surface via finite element approach, *Fractal Fract.*, **5** (2021), 119. https://doi.org/10.3390/fractalfract5030119

30. S. Rashid, S. Sultana, Y. Karaca, A. Khalid, Y. M. Chu, Some further extensions considering discrete proportional fractional operators, *Fractals*, **30** (2022), 2240026. https://doi.org/10.1142/S0218348X22400266

31. F. Mainardi, Fractional calculus, in *Some Basic Problems in Continuum and Statistical Mechanics*, Springer, Vienna, (1997), 291–348. https://doi.org/10.1007/978-3-662-03425-5_12

32. I. Podlubny, *Fractional Differential Equations*, Academic Press, San Diego, 1999.

33. W. M. Qian, H. H. Chu, M. K. Wang, Y. M. Chu, Sharp inequalities for the Toader mean of order -1 in terms of other bivariate means, *J. Math. Inequal.*, **16** (2022), 127–141. https://doi.org/10.7153/jmi-2022-16-10

34. T. H. Zhao, H. H. Chu, Y. M. Chu, Optimal Lehmer mean bounds for the nth power-type Toader mean of $n = -1, 1, 3$, *J. Math. Inequal.*, **16** (2022), 157–168. https://doi.org/10.7153/jmi-2022-16-12

35. T. H. Zhao, M. K. Wang, Y. Q. Dai, Y. M. Chu, On the generalized power-type Toader mean, *J. Math. Inequal.*, **16** (2022), 247–264. https://doi.org/10.7153/jmi- 2022-16-18

36. M. Caputo, M. Fabrizio, A new definition of fractional derivative without singular kernel, *Prog. Fract. Differ. Appl.*, **2** (2015), 73–85. https://doi.org/10.18576/pfda/020202

37. C. Li, F. Zeng, *Numerical Methods for Fractional Calculus*, Chapman & Hall/CRC, Boca Raton, 2019.

38. A. Atangana, D. Baleanu, New fractional derivatives with non-local and non-singular kernel theory and application to heat transfer model, preprint, arXiv:1602.03408.

39. A. Atangana, Fractal-fractional differentiation and integration: Connecting fractal calculus and fractional calculus to predict complex system, *Chaos Solitons Fractals*, **396** (2017), 102. https://doi.org/10.1016/j.chaos.2017.04.027

40. M. Versaci, G. Angiulli, P. Crucitti, D. D. Carlo, F. Laganá, D. Pellicanó, et al., A fuzzy similarity-based approach to classify numerically simulated and experimentally detected carbon fiber-reinforced polymer plate defects, *Sensors*, **22** (2022), 4232. https://doi.org/10.3390/s22114232

41. S. N. Hajiseyedazizi, M. E. Samei, J. Alzabut, Y. M. Chu, On multi-step methods for singular fractional q-integro-differential equations, *Open Math.*, **19** (2021), 1378–1405. https://doi.org/10.1515/math-2021-0093

42. S. Rashid, E. I. Abouelmagd, A. Khalid, F. B. Farooq, Y. M. Chu, Some recent developments on dynamical $\hbar$-discrete fractional type inequalities in the frame of nonsingular and nonlocal kernels, *Fractals*, **30** (2022), 2240110. https://doi.org/10.1142/S0218348X22401107

43. F. Z. Wang, M. N. Khan, I. Ahmad, H. Ahmad, H. Abu-Zinadah, Y. M. Chu, Numerical solution of traveling waves in chemical kinetics: Time-fractional fishers equations, *Fractals*, **30** (2022), 2240051. https://doi.org/10.1142/S0218348X22400515

44. S. Rashid, E. I. Abouelmagd, S. Sultana, Y. M. Chu, New developments in weighted n-fold type inequalities via discrete generalized $\hat{\mathrm{h}}$-proportional fractional operators, *Fractals*, **30** (2022), 2240056. https://doi.org/10.1142/S0218348X22400564

45. S. A. Iqbal, M. G. Hafez, Y. M. Chu, C. Park, Dynamical analysis of nonautonomous RLC circuit with the absence and presence of Atangana-Baleanu fractional derivativae, *J. Appl. Anal. Comput.*, **12** (2022), 770–789. https://doi.org/10.11948/20210324

46. X. B. Zhang, X. D. Wang, H. F. Huo, Extinction and stationary distribution of a stochastic SIRS epidemic model with standard incidence rate and partial immunity, *Physica A*, **531** (2019), 121548. https://doi.org/10.1016/j.physa.2019.121548

47. F. A. Rihan, H. J. Alsakaji, Analysis of a stochastic HBV infection model with delayed immune response, *Math. Biosci. Eng.*, **18** (2021), 5194–5220. https://doi.org/10.3934/mbe.2021264

48. X. Mao, *Stochastic Differential Equations and Applications*, Horwood, Chichester UK, 1997.

49. K. X. Li, Stochastic delay fractional evolution equations driven by fractional Brownian motion, *Math. Methods Appl. Sci.*, **38** (2015), 1582–1591. https://doi.org/10.1002/mma.3169

50. A. Kerboua, A. Debbouche, D. Baleanu, Approximate controllability of Sobolev-type nonlocal fractional stochastic dynamic systems in Hilbert spaces, *Abstr. Appl. Anal.*, **2013** (2013), 262191. https://doi.org/10.1155/2013/262191

51. B. Pei, Y. Xu, On the non-Lipschitz stochastic differntial equations driven by fractional Brownian motion, *Adv. Differ. Equations*, **2016** (2016), 194. https://doi.org/10.1186/s13662-016-0916-1

52. A. Atangana, S. I. Araz, Modeling and forecasting the spread of COVID-19 with stochastic and deterministic approaches: Africa and Europe, *Adv. Differ. Equations*, **2021** (2021), 1–107. https://doi.org/10.1186/s13662-021-03213-2

53. B. S. T. Alkahtani, I. Koca, Fractional stochastic SIR model, *Results Phys.*, **24** (2021), 104124. https://doi.org/10.1016/j.rinp.2021.104124

54. S. Rashid, M. K. Iqbal, A. M. Alshehri, R. Ahraf, F. Jarad, A comprehensive analysis of the stochastic fractal-fractional tuberculosis model via Mittag-Leffler kernel and white noise, *Results Phys.*, **39** (2022), 105764. https://doi.org/10.1016/j.rinp.2022.105764

55. J. M. Shen, Z. H. Yang, W. M. Qian, W. Zhang, Y. M. Chu, Sharp rational bounds for the gamma function, *Math. Inequal. Appl.*, **23** (2020), 843–853. https://doi.org/10.7153/mia-2020-23-68

56. X. Song, S. Wang, J. Dong, Stability properties and Hopf bifurcation of a delayed viral infection model with lytic immune response, *J. Math. Anal. Appl.*, **373** (2011), 345–355. https://doi.org/10.1016/j.jmaa.2010.04.010

57. D. Wodarz, Hepatitis C virus dynamics and pathology: The role of CTL and antibody responses, *J. Gen. Virol.*, **84** (2003), 1743–1750. https://doi.org/10.1099/vir.0.19118-0

58. N. Yousfi, K. Hattaf, A. Tridane, Modeling the adaptative immune response in HBV infection, *J. Math. Biol.*, **63** (2011), 933–957. https://doi.org/10.1007/s00285-010-0397-x

59. A. Murase, T. Sasaki, T. Kajiwara, Stability analysis of pathogen-immune interaction dynamics, *J. Math. Biol.*, **51** (2005), 247–267. https://doi.org/10.1007/s00285-005-0321-y

60. C. S. Holling, The functional response of predators to prey density and its role in mimicry and population regulations, *Mem. Entomol. Soc. Can.*, **45** (1965), 5–60. https://doi.org/10.4039/entm9745fv

61. B. Oksendal, *Stochastic Differential Equations: An Introduction with Applications*, 6th edition, Springer, New York, NY, USA, 2003.

62. C Ji, D. Jiang, Treshold behaviour of a stochastic SIR model, *Appl. Math. Modell.*, **38** (2014), 5067–5079. https://doi.org/10.1016/j.apm.2014.03.037

AIMS Press